External Research Report
Issue Date: 31/04/2015
ISSN: **2423-0839**

Report ER3

Seismic Improvement of Loadbearing Unreinforced Masonry Cavity Walls

Dmytro Dizhur and Jason Ingham

Project LR0458
University of Auckland funded by the Building Research Levy

1222 Moonshine Rd,
RD1, Porirua 5381
Private Bag 50 908
Porirua 5240
New Zealand

branz.nz

THE UNIVERSITY OF AUCKLAND

FACULTY OF ENGINEERING

BRANZ

Seismic Improvement of Loadbearing Unreinforced Masonry Cavity Walls

NEW ZEALAND

Final Report – 33825.001

Submitted to BRANZ April 2015




Dmytro Dizhur and Jason Ingham

Executive Summary

The main objectives of the reported research were to develop a background understanding of unreinforced masonry (URM) cavity wall type construction, to identify typically occurring failure modes, and to establish seismic retrofit solutions for URM cavity wall construction. An informative background to URM cavity walls is presented in sequence of historical development, typical construction details, and observed damage in major past earthquakes. From URM building surveys it was found that cavity walls in their original state make up approximately 40% of URM construction in New Zealand, with the remainder having solid interconnected multi-leaf walls. Based on a detailed review of 125 URM cavity wall buildings that were damaged during the 2010/2011 Canterbury earthquakes, it was concluded that unretrofitted URM cavity walls generally suffered irreparable damage due to weak mortar strength and lack of effective wall restraints. The majority (approximately ¾) of the observed damage was a result of out-of-plane type wall failures. Three types of out-of-plane wall failures that were commonly observed in cavity walls were: (1) Cantilever type failure with the entire top section of a wall or building façade collapsing (36%); (2) One-way bending type failure, which tended to occur in long spanning walls and/or walls without side support (7%); (3) Two-way bending type failure, which tended to occur in walls restrained at all boundaries (57%). In-plane damage of URM cavity walls was less widely observed (approximately ¼) compared to out-of-plane damage, and commonly included diagonal shear cracking in piers, spandrels and walls as well as to a lesser extent shear sliding on mortar bed joints or between building storeys.

It was concluded that the original cavity wall ties were typically corroded due to moisture ingress. These badly corroded wall ties further diminished the lateral seismic capacity of cavity walls and their resistance to shear and flexural actions. It was identified that the most commonly encountered ties were horse-toe steel wire ties, having a cross-section that was typically found to be significantly deteriorated due to corrosion at the mortar bed joints. Pull-out of wall ties from mortar joints was also observed.

Shake table experimental testing of four walls that closely mimicked in-situ conditions for the most commonly encountered URM cavity wall arrangements was undertaken. The dynamic testing of the walls was conducted in the as-built condition, as well as following improvement using solutions for interconnecting individual URM layers. As-built wall W1 achieved a PGA of 0.45g, while retrofitted walls W2 and W3 reached a PGA of 0.58g and 0.71g respectively, being a 30% and a 57% improvement. Wall W4 was constructed using stronger mortar and reached a 30% higher PGA (0.59g) than did as-built wall W1. The PGA achieved in retrofitted wall W4.2 was 1.00g, being 70% higher than achieved for the as-built test W4.1.

For all walls, the crack-pattern was mainly concentrated in the top quarter of the wall height. The as-built walls clearly revealed the low strength of original ties and their inability to provide composite action between the wall layers. Retrofitted walls mainly resulted in composite behaviour of the two wall layers, leading to rigid body behaviour. This rigid body behaviour was confirmed based on analysing the horizontal displacement data. Highest displacements occurred in the test walls with weak mortar.

In all as-built walls (W1.1 and W4.1), high displacements were reached at relatively small PGA values. The initial cracking was observed at approximately 0.20g, corresponding to a 3 mm mid-height displacement and a 5 mm displacement at the top of the walls. The retrofitted walls W2.1, W3.1 and W4.2 initiated cracking at 0.14g, 0.25g and 0.56g respectively, with mid-height displacements of less than 2 mm. It was shown that a simple and cost effective method of interconnecting individual cavity wall layers resulted in a significant improvement of wall performance when subjected to lateral shaking.

Contents

LIST OF FIGURES

LIST OF TABLES

1. Introduction

Loadbearing cavity (aka hollow) wall construction is a form of masonry wall construction where two layers of unreinforced clay brick masonry (URM) wall are separated by a continuous air cavity and are interconnected using some form of tie system. The cavity construction technique for loadbearing walls originated in the United Kingdom in the early 19th century and was subsequently widely adopted in New World colonies of North America and the Southern Hemisphere, with URM buildings having cavity walls being constructed in New Zealand primarily between 1880 and 1935 (Russell and Ingham 2010). The main advantage of cavity walls over solid walls (having no separation between masonry layers) of the same thickness is to provide a considerable reduction in material cost by decreasing the quantity of bricks and mortar required for construction. In addition, the air cavity between the two layers of masonry reduces penetration of the external moisture through to the inner layer and subsequently to the interior living areas. URM cavity construction also has increased fire resistance and enhanced insulation properties when compared to solid URM construction (Downing 1850).

The gravity load support system in URM cavity type buildings is typically well designed with some allowance for lateral loads generated by wind forces. However, the design of URM type buildings typically does not account for lateral loads generated by earthquake induced shaking. Hence, the seismic performance of cavity walls is frequently limited and has been repeatedly illustrated in past large earthquakes to be deficient (Page 1991; Dizhur et al. 2010; Dizhur et al. 2011)

URM cavity type construction is a well-known construction technique. However, a lack of knowledge exists in literature regarding the particular aspects of URM cavity buildings that adversely affect their earthquake performance, such as typical wall geometrical properties, wall cross-section details and diaphragm-to-wall seating arrangements, plus details of cavity wall tie configuration, spacing and condition. Currently there is also a lack documentation of the earthquake failure modes that are likely to be exhibited as a result of deficiencies in URM cavity wall buildings. Based on a review of the technical literature, no experimental studies have previously addressed the dynamic performance of URM cavity walls with original wall ties, and similarly there is a lack of reported experimental validation to support commonly adopted seismic retrofitting techniques. The study reported herein attempted to fill this knowledge gap as well as provide a database of observed critical cavity wall earthquake failure modes.

2. Background

2.1 Early use of URM cavity construction

The term ‘hollow wall’ was defined as a wall built using clay brick URM in two thicknesses with a cavity in between, for the purpose of saving materials and preserving a uniform internal dwelling temperature (Nicholson 1852). Two types of URM hollow wall construction were originally used in the United Kingdom (Hamilton 1958), with the first wall type being described as 9 inches (230 mm) thick with a thin (10 mm) cavity. The two masonry layers were originally interconnected using elongated solid clay brick headers (see **Figure 1a**), where the common size of clay bricks used for the construction of cavity walls had typical dimensions of 9 x 4.5 x 3 inches (approximately 230 x 110 x 75 mm). The second wall type consisted of an outer URM layer and an inner URM layer laid on edge, separated by a 3 inch (76 mm) cavity, and tied together using brick headers also laid on edge. This wall type was commonly referred to as Silverlock’s or Rat-Trap bond (see **Figure 1b**,**c**), although Hamilton (1958) noted that the Rat-Trap cavity wall construction technique did not gain prevalence in the United Kingdom. Cavity wall layers that are interconnected by brick headers are not easy to identify based on the bond pattern as the ends of the brick ties cannot be readily distinguished from common solid URM walls (Flemish bond pattern arrangement, see **Figure 1d**). One disadvantage of brick-tied cavity walls is that moisture can penetrate through part of the wall via the header bricks, as the air cavity cannot be continuous and the header bricks create a bridging path for moisture to transfer between the two masonry layers.

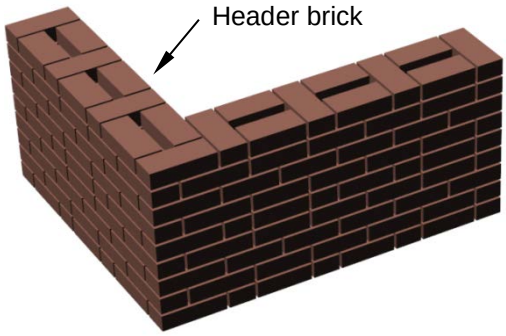

(a) Early cavity wall with slightly elongated clay brick header

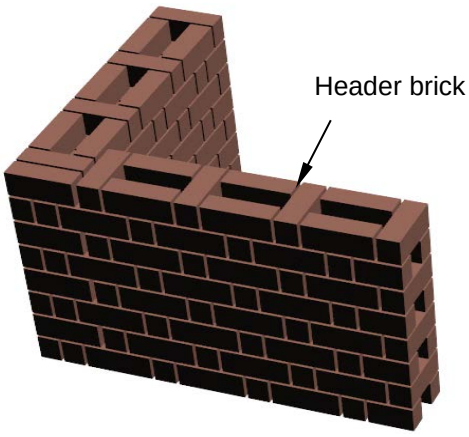

(b) Rat-trap bond

Figure 1 continues over page

(c) Rat-trap bond at Westmere Memorial Presbyterian Church**,** Whanganui

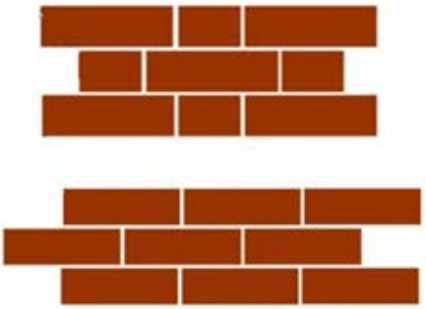

(d) Flemish bond (top) and stretcher bond (bottom)

Figure 1 – Examples of early URM cavity wall bond patterns

2.2 Evolution of URM cavity construction

In order to address the bridging path for moisture to transfer between two masonry layers via solid header bricks, one early detail was to make the header bricks bend from the inner layer downwards to the outer layer for the apparent purpose of moisture transfer prevention (Dearn 1821) (see **Figure 2**). The bent header bricks created an effective means of stopping moisture penetration and enabled the moisture to drop inside the cavity before reaching the inner masonry layer. Another early alternative was the use of extruded bricks (see A, B and C in **Figure 2b**), which were a form of bonding brick for cavity walls and were introduced in 1858. These extruded bricks were made in lengths to suit different wall thicknesses (Gwilt, 1888). Each brick was made with vertical passages through it, and had projections and grooves at each brick side, while the bedding faces had hollows sunk into them in order to prevent moisture flowing from one layer to the other. The edges of each end of the extruded brick were jagged so as to hold the external and internal wall layers more firmly together when laid in construction. This type of extruded header brick with vertical passages may be considered as more effective in moisture prevention when compared to the type shown in **Figure 1**. The authors have not yet observed such extruded brick detailing in inspected cavity walls in New Zealand.

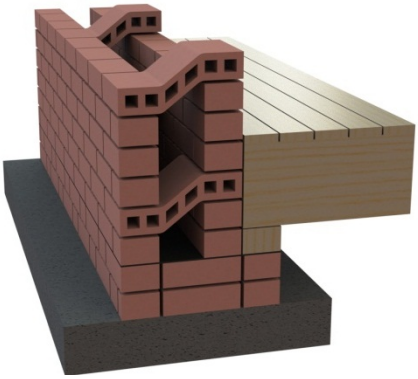

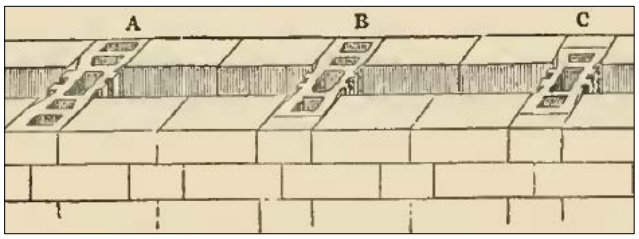

(a) Bent clay header bricks (b) Extruded clay header bricks (Gwilt, 1888)

Figure 2 – Early details of header bricks used to tie the two cavity layers together

The second type of hollow wall described by Hamilton (1958) was an evolution of the first type and used metal wall ties to interconnect the individual wall layers. The use of header bricks was rapidly superseded in the 1840s by the use of metal ties, with early metal ties typically made of cast-iron or wrought iron, either untreated or dipped in tar and sand before being laid in the wall (see **Figure 3**). The cavity walls that were interconnected using metal ties typically consisted of a Stretcher bond pattern (see **Figure 1d**). As a correspondent of the London Builder wrote in 1854:

> *The only method yet practiced to completely prevent the percolation of water from the outer surface is by means of iron stays, the two ends built into the outer and inner walls respectively, and the middle part is bent downwards, so that water cannot follow the course of the iron, but must drop to the bottom of the cavity between the walls, these stays connect the two walls so that they form one firm wall* (Lewis, 1998).

During the 1850s, metal tied brick cavity walls had been used in nearly 80 percent of the dwellings built in Southampton, England (Hamilton, 1958).

(a) Cast iron (left 2) and wrought iron (right 2) ties (reproduced from Hamilton, 1958)

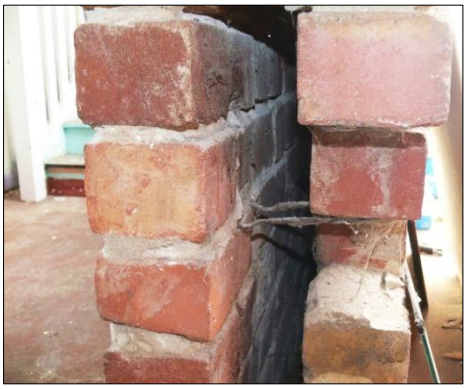

(b) Typical cavity wall cross-section showing metal ties

Figure 3 – Typical metal ties and typical cavity wall cross-section

Durability became a common issue with metal cavity wall ties because of their susceptibility to corrosion (see **Figure 4**). Hence cast-iron ties were later replaced with ties having copper welded to their surface or made of hot dipped galvanized steel. The galvanized ties had various shapes, as indicated in **Figure 5**. Double triangle (aka butterfly ties) and horse-toe ties, which are more flexible than other configurations, were mainly used for single storey domestic scale construction. Vertical twisted and fishtailed ties were more substantial in cross-section and were generally more suitable for multi-storey construction (McKenzie 2001).

(a) A rusted V-drip fishtailed tie

(b) Severe level of corrosion of cast iron tie

(c) Severe reduction of cross-section of the Horse-toe steel type ties

Figure 4 – Examples of metal tie corrosion

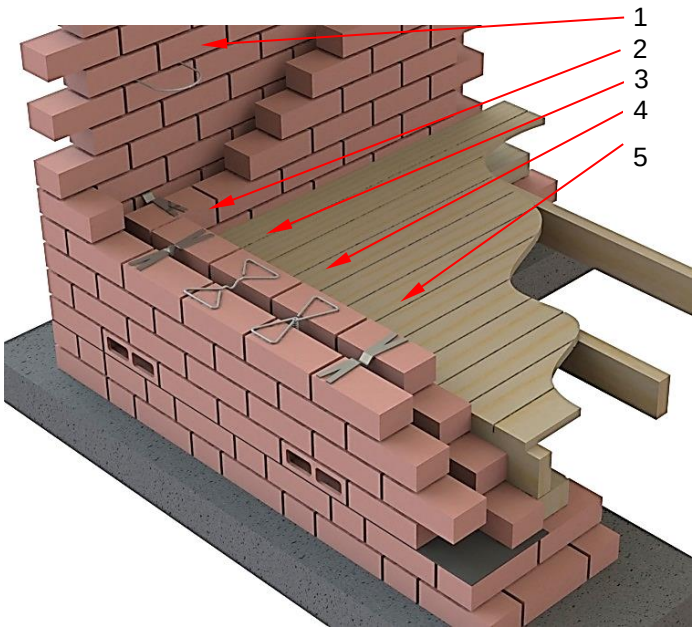

Figure 5 – Typical galvanized cavity wall ties in different configurations

Table 1 - Legend for Figure 5

Tie No. as per Figure 5	*Types of ties*
1	Horse-toe ties
2	Flat fishtailed ties
3	Vertical twist ties
4	Butterfly ties
5	V-drip flat fishtailed ties

2.3 Prevalence of cavity walls in New Zealand

The plethora of out-of-plane wall failures during the 2010/2011 Canterbury earthquake sequence revealed the extent of cavity construction in Christchurch's URM building stock. Previously cavity construction, as opposed to interconnected multi-leaf walls, was believed to be much less common in New Zealand when compared to solid wall construction. However, post-earthquake observations indicated that cavity construction was present in a large proportion of Christchurch URM buildings (see **Table 2**). The presented data is also based on surveys conducted in Auckland (Walsh et al. 2014) and a preliminary survey of limited extent undertaken in the Dunedin area.

Table 2 – Cavity type URM construction for major cities as a percent of all URM buildings

Survey region	Percent of cavity type URM construction
Auckland	40%[a] (900)
Christchurch CBD	20%[b] (370)
Christchurch outside CBD	50%[b] (180)
Dunedin	40%[c] (50)

[a] – based on study by Walsh et al. (2014)
[b] – most buildings were demolished following the 2010/2011 earthquake sequence
[c] - based on relatively small sample size of URM buildings
Note - data rounded to nearest 10. Data in parenthesis indicates sample size

3. Construction Details

3.1 Wall thickness & structural forms

In early cavity wall construction both the exterior and interior masonry layers and the cavity varied considerably in width, with the air cavity varying from less than 50 mm wide to 100 mm wide. In most buildings two single masonry leafs of brickwork would be separated by only a 50 mm cavity (see **Figure 6a**), but it was nevertheless recognised that the thicker the masonry and the wider the cavity between the leaves, the more effective the protection is against moisture penetration to the internal space, resulting in a warmer enclosed air space. In addition to cavity walls constructed of two single leaf layers, a commonly observed detail was to have a double loadbearing inner layer (see **Figure 6b**). The London Building Byelaws of the early 1920s made it compulsory for one layer to be a full brick wide (such as two leaves) and this requirement may partially explain why relatively few cavity walls were built in London at that time (Pickles et al., 2010). The use of a double-double layer wall separated with an air cavity was also observed, but less frequently (see **Figure 6c**).

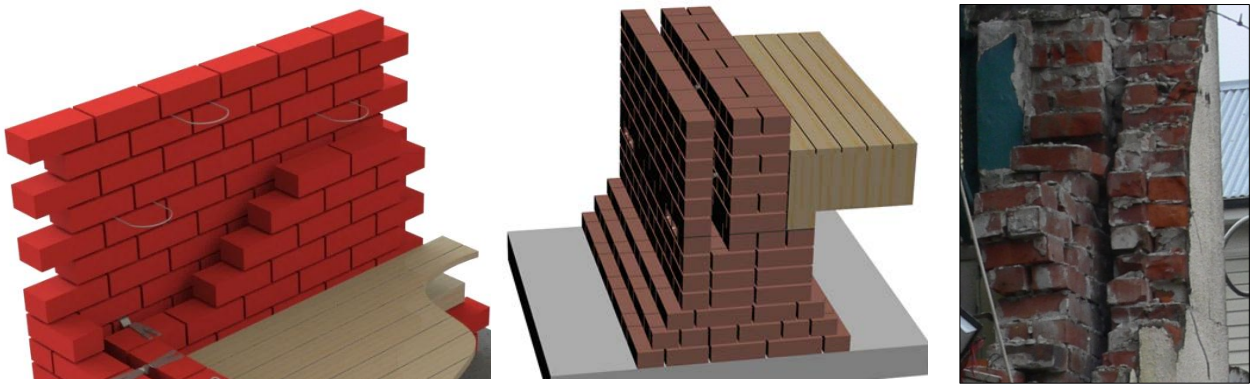

(a) Single-single masonry layers (b) Single-double masonry layers (c) Double-double masonry layers

Figure 6 – Typical cavity wall thickness arrangements

A structural frame of steel or reinforced concrete members was common in the construction of URM buildings higher than three storeys, and was often also adopted for buildings with a lower number of storeys. In this type of construction, the frame rather than the masonry walls was used to support the gravity loads on the building and the masonry merely protected the interior from the weather and resisted the spread of fire (Ritchie, 1961). Frequently the outer surfaces of spandrel beams and columns were placed in the same plane as the extension of the outer masonry layer, and the inner part of the cavity wall was constructed flush with the surfaces of the beams and columns and anchored to them, while the outer part of the cavity wall was supported on a shelf formed by a steel angle attached to a beam, usually at each floor level (**Figure 7**). The outer layer was typically connected to the inner layer by metal ties. Similar details were used when the

structural frame was made of steel members, and other connection forms were also developed and used in the 1930s (Eveleigh, 2009).

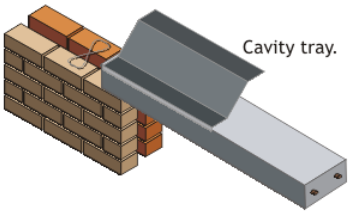

(a) Concrete lintel (with a cavity tray at times)

(b) Concrete lintel

(c) Early cavity wall with brick segmental arch in outer wall layer. Inner support could be concrete or timber

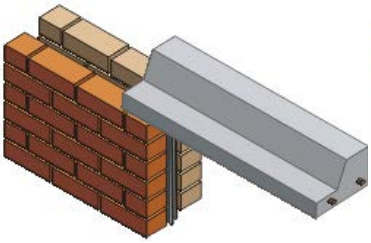

(d) Concrete lintel (covered in bitumen sometimes)

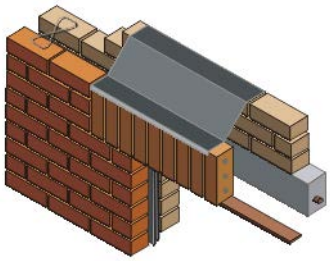

(e) Iron or steel bar below soldier course (typical 1930's detail)

(f) Soldier course with cavity tray

Figure 7 - Typical arrangement of cavity wall at a spandrel beam (reproduced from University of The West England, 2013)

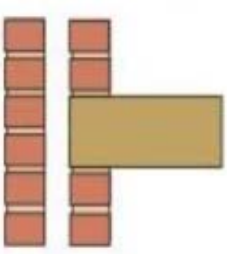

(a) Built-in to cavity

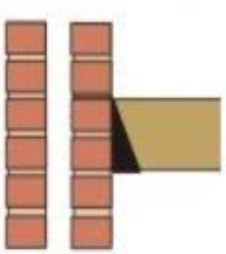

(b) Steel joist hanger

Figure 8 - 1930s cavity wall connections in the UK (Eveleigh 2009)

Gravity load from the upper floors and roof was typically carried on the inner wall layer of the wall as this mechanism enabled floor diaphragms to be kept clear of the damp external layer (see **Figure 8**), although in brick-tied construction the vertical gravity load is more likely to be shared

between both wall layers. In all cases it was necessary to ensure that the wall layers continued to be well tied together to prevent differential movement, damage during strong winds, and detachment of the outer wall layer and/or water penetration at openings (Pickles et al., 2010).

3.2 Ventilation & damp-proofing

Some cavity walls were built with a damp proof course (DPC) layer (see **Figure 9**) above ground level and often with weep-holes to allow water that penetrated the outer layer to drain outwards (Adams, 1908). In the early days of cavity construction there was much debate about whether or not the cavity should be ventilated. However, by the end of the 19th century a prevailing consensus had developed that there should be a small amount of ventilation, similar to that provided under floors, but that the cavity should be effectively sealed at openings and above the foundation (see **Figure 9a,b**). This detail provided a degree of ventilation to help any penetrating moisture evaporate away (Pickles et al., 2010).

A DPC membrane is commonly used at the bottom of the wall to prevent moisture transfer from the foundation to the wall above. Doherty (2000) conducted tests on solid URM walls with three forms of DPC construction, namely standard, centred, and slip joint. Static testing suggested that the coefficient of friction varied from 0.1 to 0.6, with the average being 0.5. Shake table tests showed that the coefficient of dynamic friction was up to 20% less than the coefficient of static friction. It is considered reasonably conservative to assume a static coefficient of friction equal to 0.45 between DPC and masonry.

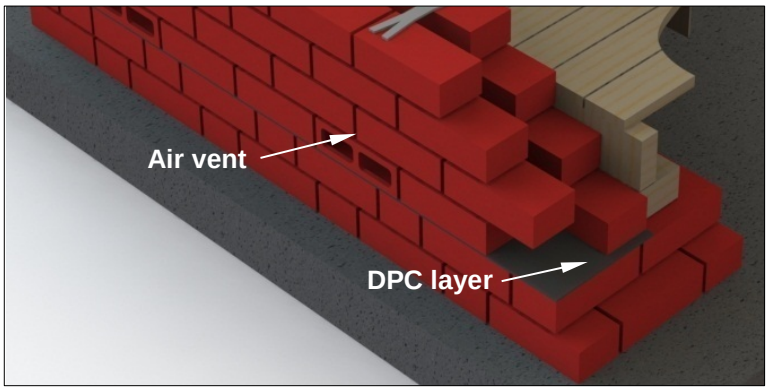

(a) Air bricks (vents) and DPC layers

Figure 9 continues over page

(b) Typical cavity wall air vents

(c) Exterior cavity wall with brick removed, exposing the lead damp-proof course and air gap cavity

Figure 9 - Air bricks (vents) and DPC layers

3.3 Floor diaphragm-to-wall connection details

The response of a cavity wall structure when subjected to lateral loads is dependent on the effectiveness of various diaphragm-to-wall seating arrangements. Detailed observations were made during demolition of NZ URM buildings with cavity type construction (mainly located in Christchurch), where the connection details between the inner masonry layer and diaphragms were exposed. The three most prevalent types of floor diaphragm-to-wall seating arrangements for cavity walls were documented and are presented below.

The type-1 diaphragm-to-wall seating arrangement (see **Figure 10**) consists of a concrete beam (reinforced with steel bars in most cases) resting on the inner loadbearing layer of the cavity wall. The outer layer of the wall extends continuously and is interconnected to the loadbearing inner layer using steel cavity ties. Timber floor joists are supported on the ledge that is typically formed due to a reduction of wall thickness with increasing floor height. This seating arrangement is prone to a cantilever type failure when subjected to earthquake induced shaking because the only connection between the two masonry layers is from the wall ties, which cannot develop flexural and shear resistance. Flexible floor or roof diaphragms, observed in most cases, can also contribute to the susceptibility of a cavity wall to fail in the out-of-plane direction due to excessive diaphragm displacement.

The type-2 seating arrangement shown in **Figure 11** has similar details to Type-1, with the concrete beam extending over the inner and outer layer of the cavity wall. The external layer of the wall is then continued from above the concrete beam for the subsequent storeys. In a typical two-storey cavity wall building, the concrete ring beam that usually sits at first floor level can be considered a fixed restraint for the cavity wall underneath. Due to the presence of a concrete ring beam, the two masonry layers underneath remain undamaged in most cases because the extra axial load from the weight of the concrete beam significantly reduces the risk of out-of-plane collapse plus the benefits of arching action that can develop when a rigid boundary restraint is

provided. The overall slenderness ratio of the cavity wall is lower than that of a solid masonry wall, which leads to greater stability. Therefore the Type-2 connection is less susceptible to out-of-plane failure when compared to Type-1.

Figure 12 shows the Type-3 seating arrangement where the masonry layers run continuously from ground to roof top. Cavity walls with this structural arrangement seldom have any anchorage systems into the floor diaphragms and usually are earthquake-prone as a result.

(a) RC beam on inner wall layer

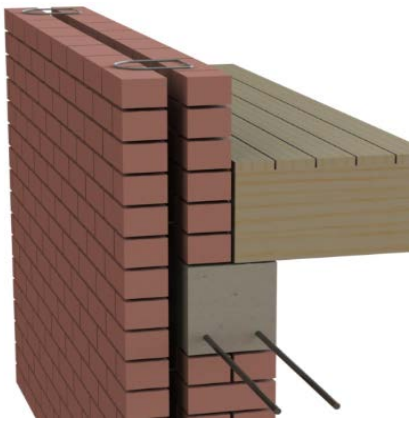

(b) Schematic showing Type-1 connection

Figure 10 - Floor diaphragm-to-wall connection Type-1

(a) RC beam extending across both inner and outer wall layer

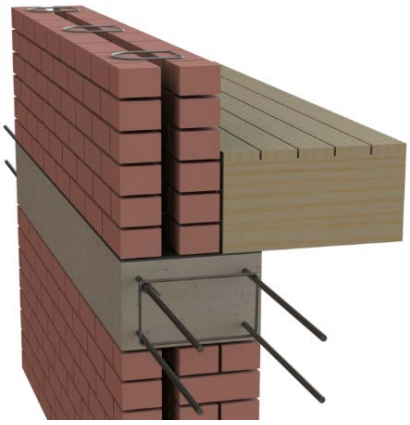

(b) Schematic showing Type-2 connection

Figure 11 – Floor diaphragm-to-wall connection Type-2

(a) Continuous outer and inner wall layer

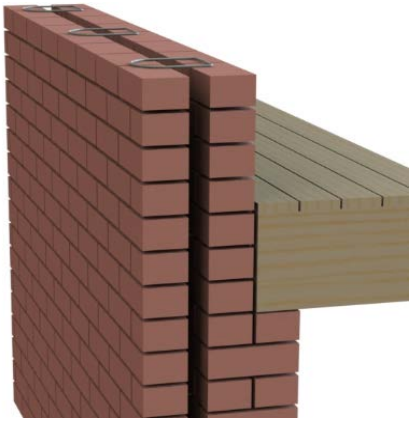

(b) Schematic showing Type-3 connection

Figure 12 - Floor diaphragm-to-wall connection Type-3

3.4 Roof diaphragm-to-wall connection and parapet details

In addition to floor-to-wall seating arrangements, the most prevalent types of roof seating arrangements and parapet types were observed during building demolitions. The most commonly encountered configuration for the connection between the roof diaphragm and wall is shown in **Figure 13**. Often this connection type provides some degree of restraints to the top of the wall, from timber members that extend from the soffit of the roof framing system. Compared to other types of original seating arrangement of the roof diaphragm, the arrangement shown in **Figure 13** reduces the risk of cavity walls failing in an out-of-plane cantilever type collapse.

Unreinforced masonry parapets are a non-structural and decorative element that extends above the roof around the perimeter of a building. In the Christchurch CBD region it was observed that approximately 50% of parapets on the top of cavity wall type URM buildings were of cavity type construction. It was probable that parapets constructed of cavity walls were a consequence of builder preference or for consistency of the cavity construction method.

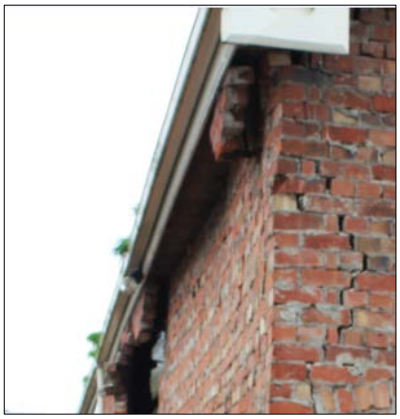

(a) Photograph showing detail

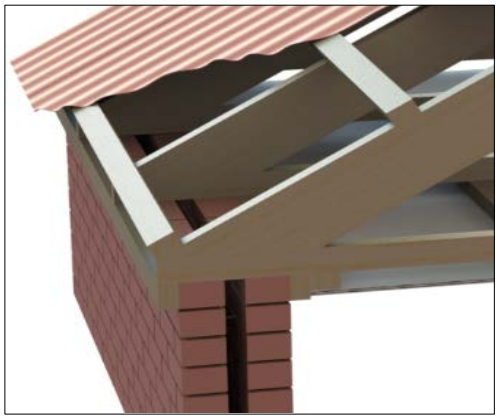

(b) Schematic showing detail

Figure 13 – Typical roof diaphragm-to-wall connection

A solid wall type parapet over a cavity wall is shown in **Figure 14**, where the roof framing seating arrangement is located at the transition from cavity to solid construction, and a continuous cavity type parapet is shown in **Figure 15**, where the cavity construction is full height, including the parapet with capping and flashing over the top part of the wall. The roof framing seating is typically pocketed into the interior layer of the wall. A cavity type parapet on top of a concrete beam and roof seating arrangement can be observed in **Figure 16**.

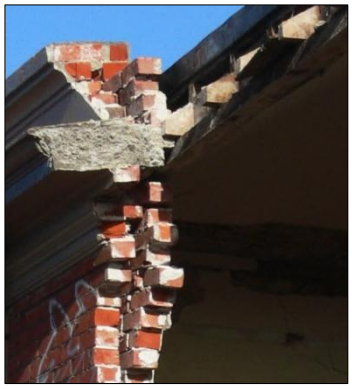

(a) Photograph showing detail

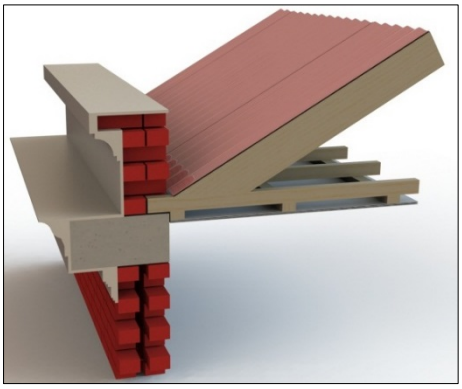

(b) Schematic showing detail

Figure 14 - Solid wall type parapet over cavity wall

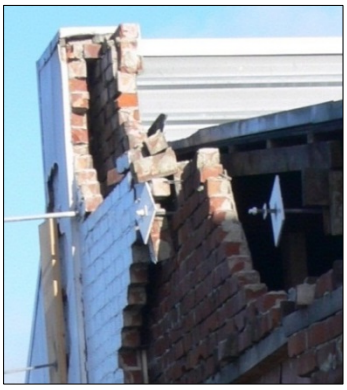

(a) Photograph showing detail

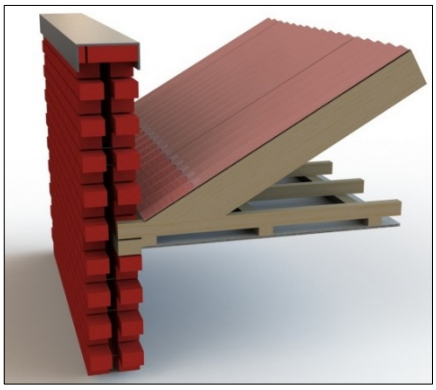

(b) Schematic showing detail

Figure 15 - Continuous cavity type parapet

(a) Photograph showing detail

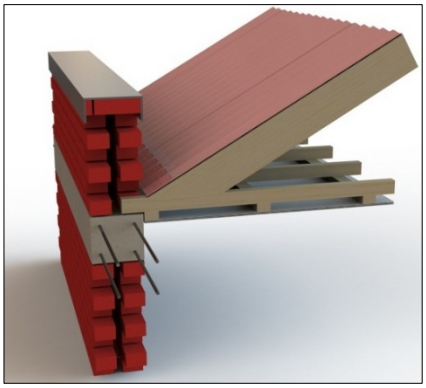

(b) Schematic showing detail

Figure 16 - Cavity parapets with a concrete beam at roof level

4. Site Investigations

A series of site investigations was conducted on existing cavity wall buildings located in Auckland and Christchurch. These detailed building inspections were performed by first seeking and obtaining building access permission from building owners/tenants. Buildings with URM cavity wall construction were selected to be spatially distributed throughout the Auckland region, with site visits mainly conducted in 15 buildings located on Ponsonby Road and Dominion Road in Auckland, where both streets have numerous historic buildings that were constructed before the 1930s. Appropriate inspection tools such as boroscope cameras, ferro-scanners and ground penetrating radar (GPR) were utilised during the detailed site investigation stage. A review of a photographic database of 125 URM buildings with cavity type wall construction and sample collection of URM buildings damaged during the 2010/2011 Canterbury earthquakes was also undertaken.

4.1 Mortar

Mortar that was used as a bonding material in early cavity wall construction was generally composed of lime and clean sand. The use of lime rather than cement (as used in modern cavity wall construction) resulted in relatively weak compressive strength of the mortar and hence a low bond strength. Based on the investigations undertaken following the 2010/2011 Canterbury earthquakes, it was observed that mortar from building debris, typically lime based mortar, possessed low average compressive strengths of 0.45 MPa (Dizhur et al. 2011). The weak mortar can be readily crushed when subjected to finger pressure, as illustrated in **Figure 17a**.

(a) Low mortar strength (b) Common mortar loss

Figure 17 – Examples of ultra-weak lime based mortar

The workmanship quality control for early cavity wall buildings appears to have been highly variable at the time of construction. As a result of poor workmanship, such as failure to fill the vertical mortar joints, water penetration and mortar degradation is commonly encountered. In some cases, the mortar simply dried-out instead of hardening and never adhered to the bricks

(Dickey, 1974). **Figure 17b** shows a cavity wall building in Auckland that exhibited a typical example of mortar loss due to dehydration and wash out.

4.2 Cavity wall ties

Cavity wall tie typologies, spacing and condition were parameters that were documented during the surveys by using direct inspection where possible and using a borescope camera (see **Figure 18**). Post-earthquake observations of 47 damaged Christchurch buildings having URM cavity wall type construction, and where tie typologies were visible, showed that horse-toe (aka square, see **Figure 4** & **Figure 5**) metal ties were the most common type and were used in 54% of the assessed buildings, as presented in **Figure 19**. In addition, from a review of a photographic database of 47 (out of 125) URM buildings with cavity type walls that were damaged during the 2010/2011 earthquakes and where tie spacing was able to be identified, the most common spacing was identified as:

- Horizontally approximately 690 mm (every three bricks within a course)
- Vertically approximately 450 mm (approximately every six courses)

These tie spacing findings were confirmed by utilising Ferro-scanners and ground penetrating radar (GPR) during the detailed site investigation stage of selected buildings located in Auckland.

(a) Use of Borescope camera

(b) Existing cavity ties

Figure 18 - Cavity wall tie investigations in Auckland using a borescope camera

The wall ties in most inspected buildings were found to have some level of corrosion, and cases of missing ties were identified. These observations were attributed to the fact that metal ties are highly susceptible to corrosion when exposed to moisture which is usually captured in the cavity and ventilated out gradually. Moreover, most cavity wall buildings in New Zealand have existed for over one century, and the repetitive moisture ingress on the metal wall ties has led to a significant extent of corrosion. Even though some metal wall ties were dipped with protective coatings before being laid during original construction, due to progressive loss of the coating, corrosion still occurred (see **Figure 4** and **Figure 20** for photographic examples).

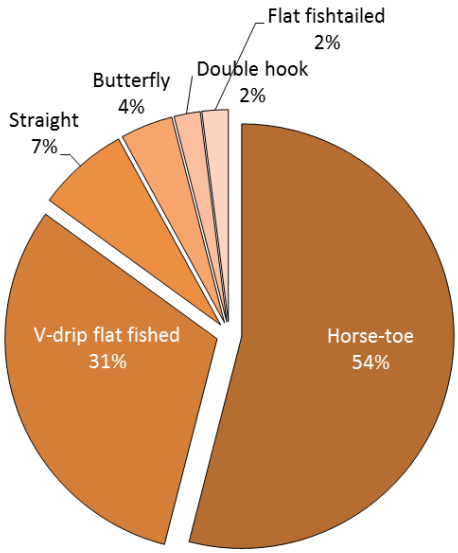

Figure 19 - Type of cavity wall ties (see **Figure 5**) from 47 buildings that were damaged during the Canterbury earthquakes

4.3 Wall tie tests

A set of cavity wall ties was collected from the debris of the demolished URM cavity wall buildings in Christchurch during a comprehensive post-earthquake survey of the URM building stock. The condition of the collected ties was found to be poor and mostly rusted. The ties were manually straightened and cut into appropriate section lengths (see **Figure 20**) that could be tested in direct tension.

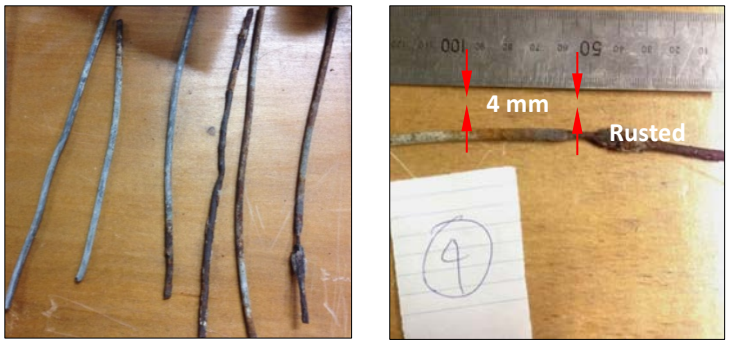

Figure 20 – Collected wall tie samples for tensile testing

It was identified that the un-corroded tie sections sustained approximately 6.0 to 6.5 kN at tension failure. However, the weakest sample, that had a significant amount of corrosion with severe material loss of the cross-section, failed at approximately 2 kN. A total of 12 tensile tests were conducted.

5. Seismic Performance & Risks

It is well known that the devastating Hawke's Bay earthquake in 1931 occurred before the introduction of the first seismic code in New Zealand, and Dowrick (1996) reported that many non-residential URM buildings were severely damaged after being subjected to strong ground shaking. Construction of URM buildings in New Zealand, including cavity wall construction, declined dramatically thereafter due to their observed inadequate seismic performance.

Ambiguity of structural analysis exists regarding whether or not a cavity wall section should be considered as one section or as two independent sections of separated masonry layers. Monk (1960) reported that the weakness in strength of a cavity wall compared to its equivalent solid counterpart was attributed to the inadequate ability of wall ties to develop flexural-shear resistance between the two masonry wall layers. The high slenderness ratio of each masonry layer, combined with the ineffectiveness of the cavity wall ties, would lead to differential movements of the two masonry wall layers. Analysis based on two sections where interconnection contributions of the ties are neglected is typically considered as a conservative analysis approach. In areas where past earthquakes have occurred, such as the 1989 Newcastle earthquake and the 2010/2011 Canterbury earthquakes, severe damage to URM cavity wall type buildings was observed and documented. The performance of URM cavity wall construction in these two earthquakes is considered below

5.1 1989 Newcastle Earthquake

On 29 December 1989 a magnitude 5.6 earthquake struck the city centre of Newcastle, Australia, at a depth of approximately 11 km. It was reported by Griffith (1991) that the majority of buildings that suffered severe damage were of URM construction. Common failure modes were observed which indicated the shortcoming of the Australian seismic code at the time of the earthquake. Out-of-plane failure of URM construction, typically cavity walls, was critical in terms of structural stability and safety issues and collapse of the outer masonry cavity wall layer due to wall bending failure was commonly encountered. Another important observation following the 1989 Newcastle earthquake was that cavity wall ties were often corroded, resulting in a poor connection between the two masonry wall layers. Therefore, the capacity of wall ties to transfer lateral load was significantly deminished due to cross-sectional reduction.

Additionally, it was reported that the scale of damage incurred in the 1989 Newcastle earthquake was mainly attributed to the poor quality of masonry construction, including inadequate structural detailing and poor mortar strength (Page 1996). Although Australia is regarded as a low seismic hazard area, following the 1989 Newcastle earthquake there has been modification of Australian seismic codes and implementation of detailing requirements to meet higher earthquake demands.

5.2 2010/2011 Canterbury Earthquakes

In the early morning of 4 September 2010 the region of Canterbury, New Zealand, was subjected to a magnitude M7.1 earthquake. The epicentre was located near the town of Darfield, 40 km west of the city of Christchurch. A magnitude M6.3 aftershock on 22 February 2011, although of a smaller magnitude, produced peak ground accelerations in the Christchurch region that were substantially greater than those measured during the 4th September earthquake. Whilst in September 2010 most earthquake shaking damage was limited to unreinforced masonry buildings, in February 2011 all types of buildings sustained damage (Dizhur et al. 2010; Dizhur et al. 2011). A photographic database of 125 URM buildings with cavity type wall construction damaged during the 2010/2011 Canterbury earthquakes allowed an opportunity to study and categorise frequently occurring failure mode types. **Figure 21a** shows in-plane shear cracking of a masonry pier, and a stair-stepped failure plane through mortar bed joints that indicates weak mortar strength. **Figure 21b,c** shows diagonal shear cracking of a URM cavity wall with significant sliding occurring along the weak mortar bed joints. Similarly, shear cracks can occur in masonry spandrels.

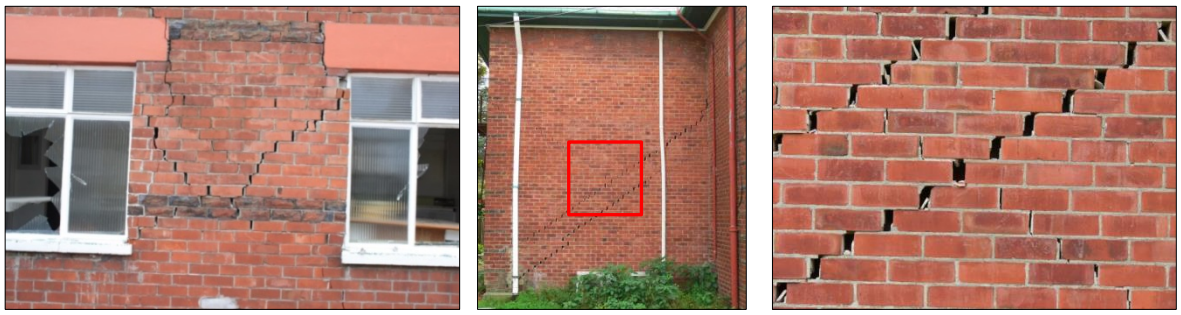

(a) Diagonal shear cracking in pier

(b) Diagonal shear cracking in wall

(c) Close up of (b)

Figure 21 - Examples of typical in-plane shear failure

In contrast to the in-plane type of wall failure, out-of-plane failure causes most of the devastating structural damage in cavity wall buildings. Post-earthquake observations from damaged buildings have resulted in out-of-plane failure mechanisms being classified into three types: (1) one-way bending (vertical bending of the wall); (2) two-way bending, and (3) cantilever response. An example of one-way bending is shown in **Figure 24** where horizontal cracking may be initiated at top and bottom and at approximately mid-height of the cavity wall whilst the wall side supports are ineffective in resisting flexural and shear actions (see **Figure 25** for another example).

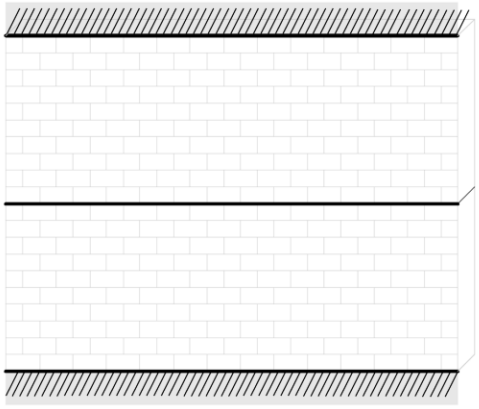

(a) Schematic example of one-way bending type failure

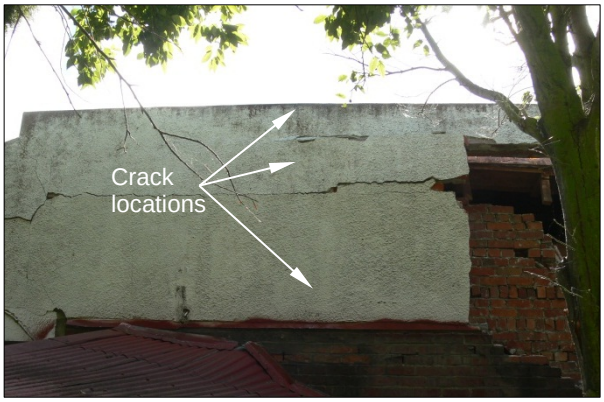

(b) Example of one-way bending type failure

Figure 22 – Out-of-plane one-way bending type failure

Two-way out-of-plane bending type failure is frequently encountered in URM walls that are subjected to earthquake induced shaking. Due to a combination of factors including boundary conditions and weak mortar strength, a typical U-shaped failure plane typically forms in the top portion of the wall (see **Figure 23** and **Figure 26** for more examples).

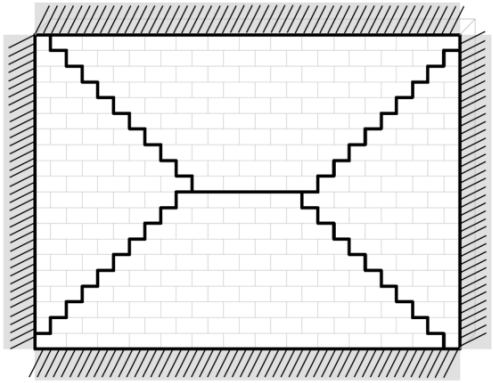

(a) Schematic example of two-way bending type failure

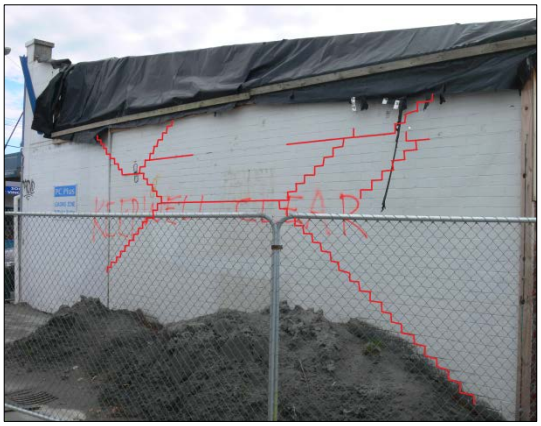

(b) Two-way typical cracking pattern (highlighted in red for clarity)

Figure 23 – Out-of-plane two-way bending type failure

Depending on the support conditions at the top and bottom of a wall, the failure mode may be a cantilever type (for example **Figure 24**) with the entire top section of a wall collapsing. For long spanning walls with an unrestrained top portion of the wall, a U-type wall failure typically occurred extending the full height of the wall as shown in **Figure 24**c,d. When the top section is well connected to the diaphragm, failure may occur in vertical or two-way bending.

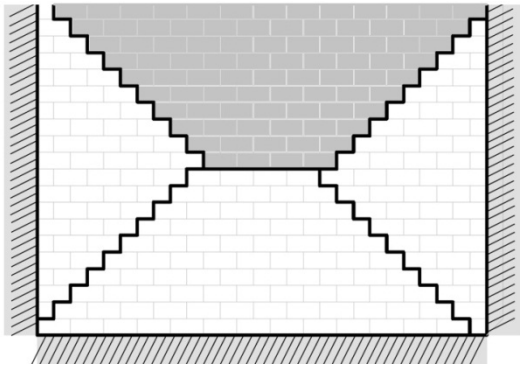

(a) Schematic example of shorter spanning wall with unrestrained top boundary support

(b) Short spanning cavity walls with unrestrained top boundary support (highlighted in red for clarity)

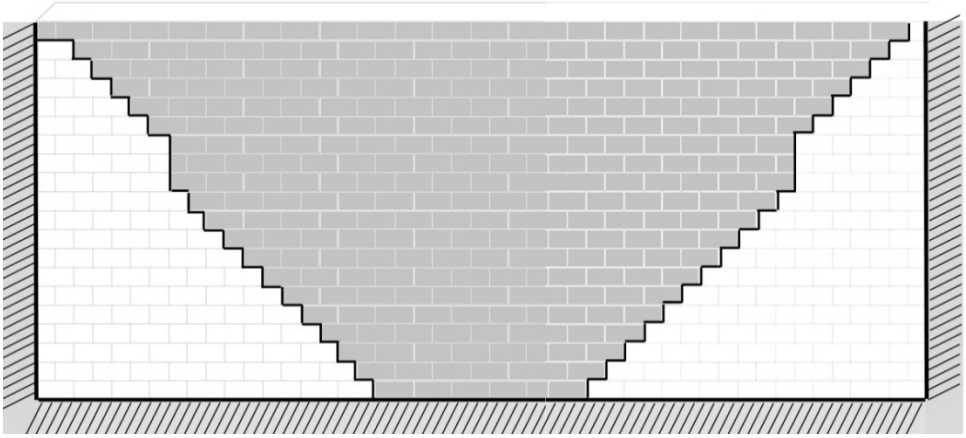

(c) Schematic example of cantilever U-type wall failure for long spanning walls

(d) Example of cantilever U-type wall failure for long spanning walls

Figure 24 – Out-of-plane cantilever U-type wall failure

More examples of out-of-plane failures observed following the 2010/2011 Canterbury earthquakes are illustrated in **Figure 25**, **Figure 26** and **Figure 27**.

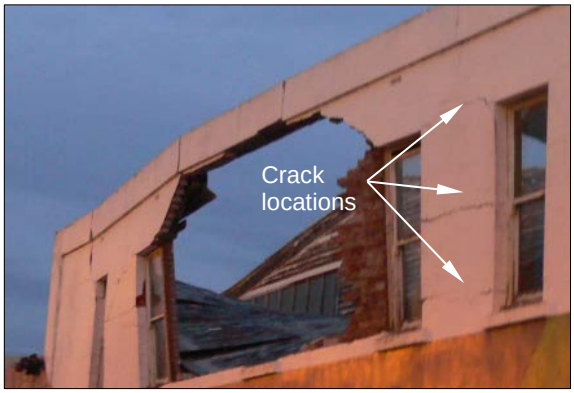

Figure 25 - Typical one-way bending example

(a) Typical two-way cracking pattern - onset of collapse of top portion

(b) Collapse in two-way bending of a cavity wall of two single leafs

(c) Typical two-way bending collapse of outer layer

(d) Side view of wall displacement - 1

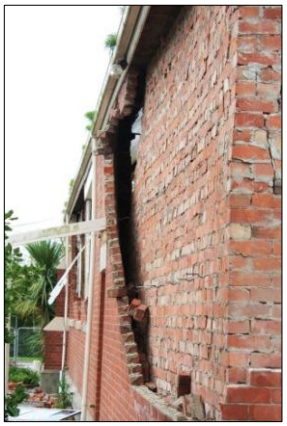

(e) Side view of wall displacement - 2

(f) Example of combined failure modes

(g) Collapse in two-way bending of a wall with two single leafs - 1

(h) Two-way bending collapse of wall having two single leafs- 2

(i) Two-way bending collapse of wall having two single leafs - 3

Figure 26 - U-shape two-way bending failure

Figure 27 – Comparison of two cavity walls. Weak lime mortar with badly corrode cavity ties and poor top restraint (right), cement mortar and adequate top support, cavity tie condition unknown (left)

5.2.1 Frequency of failure mode occurrence

It was found that 20% (125) of 627 buildings surveyed following the Canterbury earthquakes were of URM cavity type construction. It is also noted that the majority of cavity wall buildings were found outside the Christchurch CBD region where the proportion of cavity construction reached almost 50%. **Figure 28** shows the estimated percentage of in-plane and out-of-plane failure modes based on detailed observations made for the 125 cavity wall buildings located in Christchurch where sufficient photographic data exists from the earthquake reconnaissance. The percentage of each failure mode was counted by the number of occurrences, such as number of walls rather than number of buildings.

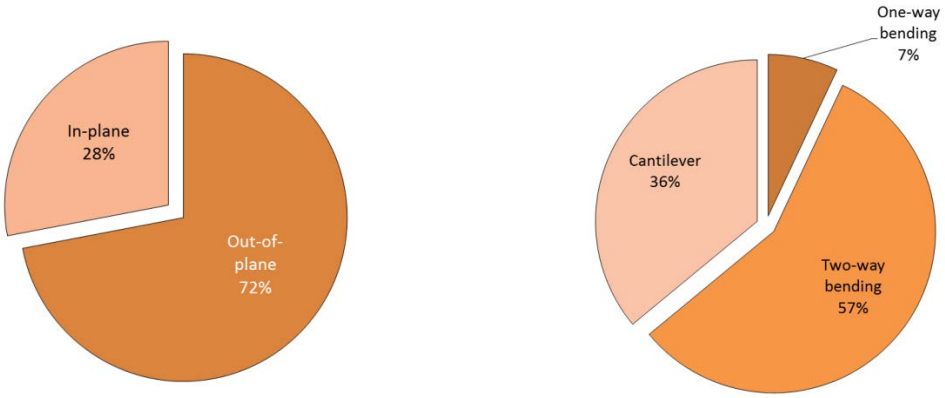

(a) Frequency of failure mode occurrence

(b) Type of out-of-plane failure mode occurrence

Figure 28 - Failure mode observation for cavity walls

5.2.2 Gable end wall failures

Gable end walls were common architectural features of early NZ churches constructed of unreinforced masonry bricks. The issue of instability of gable end walls was found to be more critical in cavity wall buildings without effective end restraints. A large percentage of gable wall failures were reported following the Canterbury earthquakes, principally due to lack of effective restraining mechanisms. Another factor that may influence the response behaviour of a cavity wall when subject to out-of-plane action is the end constraint condition, as a cavity wall with lateral end restraints possesses higher strength and stability than that with flexible end restraints.

The difference in seismic performance of gable end cavity walls is illustrated through a comparison between **Figure 29a** and **Figure 29c**. In **Figure 29b** the top of the cavity wall was poorly restrained, resulting in complete collapse of the gable end wall with failure being initiated from the top of the wall as indicated by the absence of bricks attached to roof purlins. In contrast, a more effective restraint condition is shown in **Figure 29c**, where the gable end wall suffered only partial collapse. Both ends of the gable end wall remained undamaged whilst the middle section failed, possibly due to an increasingly high slenderness ratio towards the centre for a gable end wall.

(a) Gable end walls – cantilever failure (no top restraint)

(b) Gable end walls - full collapse cantilever failure (no top restraint)

(c) Gable end walls – partial collapse (perimeter top restraint)

Figure 29 - Gable end wall failures

5.2.3 Building corner failures

It was frequently observed that the corners of buildings sustained concentrated damage and subsequent collapse (see **Figure 30**).

(a) Corner failure - 1 (b) Corner failure - 2 (c) Corner failure - 3

Figure 30 – Examples of building corner failures

5.2.4 Other observations

It was observed that some URM cavity type buildings sustained a wide range of failure modes including a mixture of in-plane damage to walls, piers and spandrels, out-of-plane and corner failures (**Figure 31**).

Figure 31 - Mixture of observed failure modes

6. Shake Table Experimental Testing

Shake table experimental testing of four walls that closely mimicked in-situ conditions for the most commonly encountered URM cavity wall arrangements was undertaken. Wall W1 was constructed in the as-built condition while walls W2 and W3 replicated retrofitted walls. Wall W4 was first tested in the as-built condition and then retrofitted and retested. These dynamic tests were performed on a dedicated shake table capable of applying sinusoidal horizontal loading. This experimental program added to the associated platform of knowledge reported in earlier sections of this report and provided the research team with the needed data to validate/improve currently available assessment techniques for URM buildings with cavity type walls when loaded in their out-of-plane direction in either original as-built or seismically improved condition. Detailed description of the tested cavity walls, experimental results, observations and discussions are presented below.

6.1 Test walls

All test walls were constructed in a running bond pattern using recycled clay bricks and with a mortar joint thickness of approximately 10-15 mm. The single-single masonry layer arrangement was previously identified as commonly occurring and hence was adopted for the shake table experimental testing. All walls were constructed on a shake table platform and left to cure for at least 28 days prior to testing. Two different mortar mixes were used for the construction of the test walls, being 0:1:3 (W1-W3) and 1:2:9 (W4) (cement:lime:sand) by volume.

All test walls were constructed with wire cavity ties interconnecting the masonry layers in order to simulate the ‘as-built’ condition that would be typically encountered in an actual vintage URM cavity wall building. Cavity wall ties were folded into the horse-toe wire tie geometry with notches cut into the wire (see **Figure 32a**) to simulate the rusted deteriorated condition of typical ties, as previously reported in Section 3.6, and were laid based on the most common tie arrangement that was observed in surveys, being two ties per row (600 mm) and one row of ties for every six masonry courses (450 mm) (see **Figure 32b**).

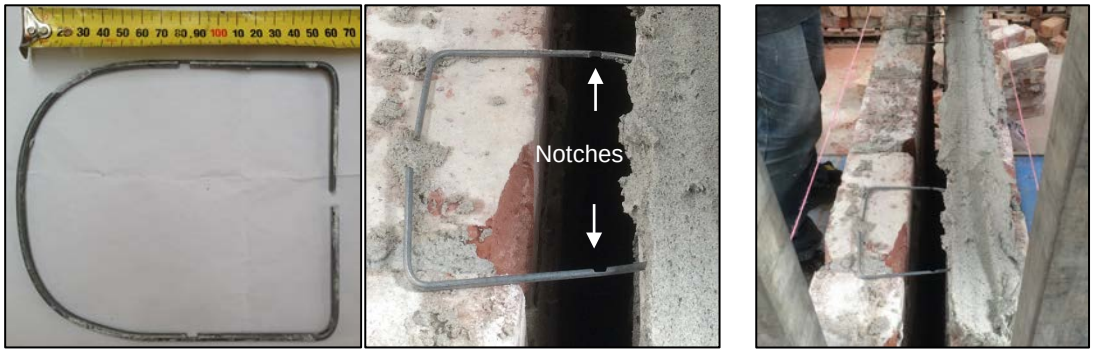

(a) Notched ‘original’ wall wire ties (W1) (b) Tie placement (W1)

Figure 32 – Replicated wire ties using notched 4 mm diameter steel wire installed in all test walls

Table 3 summarises the geometrical properties of the tested walls. All test walls were 1190 mm wide. Wall W1 was tested in the as-built condition to serve as the control and allow the level of performance improvement in strength and displacement capacity to be quantified for retrofitted W2 and W3 walls. Wall W4 was first tested in the as-built condition (W4.1) and then retrofitted with additional ties and retested (W4.2). Typically two tests were conducted for each wall (except wall W3 where only one test was undertaken). The first test (denoted as W#.1) was conducted where the table acceleration was increased incrementally (see Section 6.4.1) up to a point of wall cracking and initiation of rocking and the test was stopped. For the second test (denoted as W#.2) the table acceleration was increased incrementally up to the point of wall collapse.

Table 3 - Cavity wall test matrix

Wall ID	Test ID	Height (mm)	Total wall Thickness (mm)	Mortar mix	Retrofit type	Retrofit tie spacing, V & H (mm)
W1	W1.1	3000	270	0:1:3	Original wire ties	V - 450 H - 600
	W1.2					
W2	W2.1	3000	270	0:1:3	Φ12mm screws (Type 1)	V - 600 H - 600
	W2.2	2800				
W3	W3.1	3000	270	0:1:3	Φ12mm screws (Type 1)	V - 300 H - 600
W4	W4.1	3000	270	1:2:9	Original wire ties	Two ties per row and every 6 courses per row
	W4.2				Φ 8mm screws (Type 2)	V - 300 H - 600

1:2:9 - cement : lime : sand; Φ – diameter in mm; V – vertical spacing; H – horizontal spacing; All test walls were 1190 mm wide.

6.2 Retrofit procedure

Based on previous airbag testing of cavity walls (BRANZ LR0441 report, Ingham 2014 et al), it was summarised that of three types of retrofit techniques considered (namely stainless steel helical rods, chemical ties and mechanical screw ties, shown in **Figure 33**), the Φ12 mm mechanical screw ties were the most effective retrofit solution in terms of increasing the out-of-plane capacity of cavity walls, and hence mechanical screw ties were adopted for use in this experimental shake table study.

(a) Stainless steel helical rods | (b) Adhesive ties | (c) Steel screws Φ12mm (Type 1) | (d) Steel screws Φ8mm (Type 2)

Figure 33 – Considered retrofit techniques

Two types of mechanical screw ties were considered, with the first type being a product that was originally commercially developed to be used for anchoring into concrete substrate. The mechanical screw consisted of a 12 mm diameter steel threaded shank with a length of 230 mm (see **Figure 33c**). The screws had a total threaded length of 160 mm and a hexagonal washer type head. These screws were installed in walls W2 and W3 using a pre-drilled 12 mm diameter hole in both wall layers. When installed, the tip of the screws reached at least half depth of the bricks on the opposing masonry layer. The installation process and final appearance is shown in **Figure 34a-d**.

The second type of mechanical screw tie was specifically developed to be used as a cavity tie in clay brick masonry walls. The mechanical screw consisted of an 8 mm diameter steel threaded shank with a length of 240 mm (see **Figure 33d**). The screw has a fully threaded length and a Torx type screw head which allows the head of the fastener to be relatively small for the required torque. The diameter of the screw was selected in order to provide sufficient shear transferring capacity between the two wall layers and the thread pattern was adopted in order to optimise direct pull-out capacity and reduce the required installation torque. In wall W4 these screws were installed into a pre-drilled 7 mm diameter hole in both wall layers. The installation process and final appearance is shown in **Figure 34e,f**.

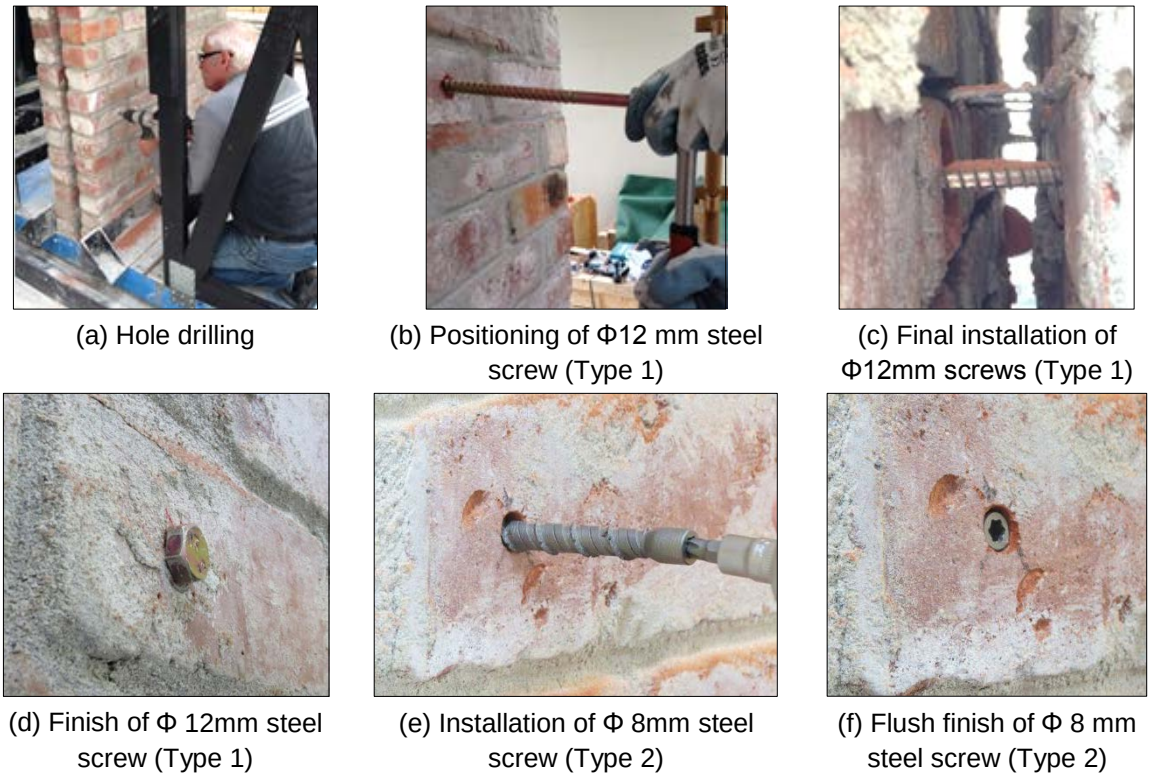

(a) Hole drilling

(b) Positioning of Φ12 mm steel screw (Type 1)

(c) Final installation of Φ12mm screws (Type 1)

(d) Finish of Φ 12mm steel screw (Type 1)

(e) Installation of Φ 8mm steel screw (Type 2)

(f) Flush finish of Φ 8 mm steel screw (Type 2)

Figure 34 - Installation process of retrofit steel screw ties

For walls W2 and W3 the spacing arrangement for Type 1 screws was adopted as shown in **Table 3**. Note that in all retrofitted walls, two screws were installed per row and each screw was 300 mm

from the nearest edge, resulting in a 600 mm spacing. For wall W4, Type 2 screws were used with 300 mm vertical spacing and 600 mm horizontal spacing respectively (see **Figure 35**).

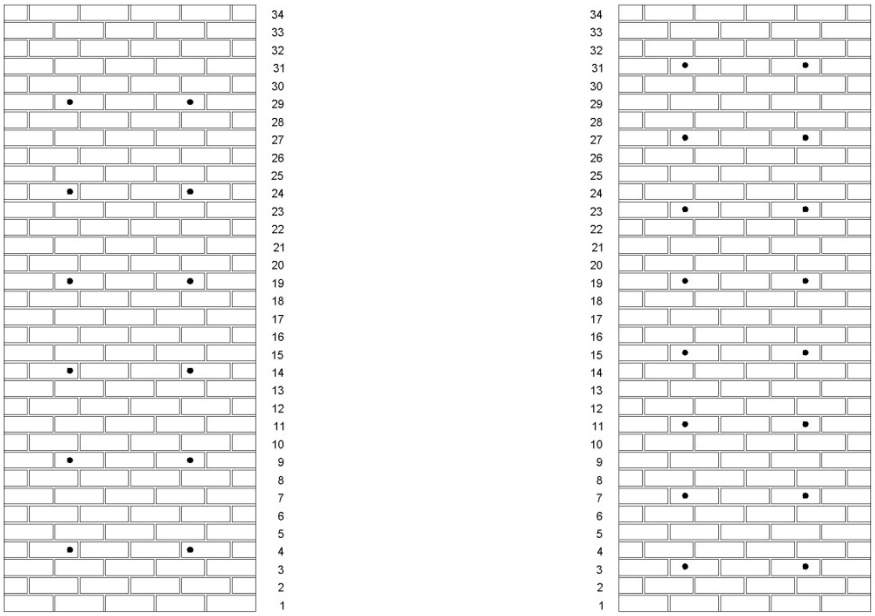

(a) (b)

Figure 35 – Position of retrofit screw ties

6.3 Material properties

All tested walls were constructed using recycled vintage clay bricks obtained from a demolished vintage URM building. The original mortar was removed and the surfaces of the bricks were prepared for new mortar before being reused in the test substructure. The bricks were estimated to be 80 years old as the demolished building was known to have been constructed in the 1930's. Recognising that within a building there is significant variability in brick properties, the reuse of vintage bricks introduced realistic material variability into the tests. Brick dimensions were of standard size (230L × 110W × 75H mm) that is commonly encountered in NZ heritage construction (Russel 2010).

Random samples of recycled bricks were taken during the construction phase and tested in compression (ASTM 2001b). Masonry prisms were built during construction of the walls using randomly selected bricks, and tested in compression and flexural bond. All material tests were conducted according to ASTM standards (ASTM 2001a; ASTM 2001c; ASTM 2002; ASTM 2003). The results of these material tests are shown in **Table 4**. The large variability in material strengths was considered acceptable because of the real variation in material properties in existing URM buildings.

A weak mortar mix of 0:1:3 (cement:lime:sand) with an average compressive strength of 0.25 MPa was selected for walls W1-W3 to simulate severe weather deteriorated mortar in vintage URM buildings (see section 4.1), whereas a mortar mix of 1:2:9 (cement:lime:sand) was selected for wall W4 to simulate vintage cavity walls with moderate mortar strength. Portland cement was becoming more widely available in the early part of the 20th Century when URM was the building material of choice in NZ, as was hydrated lime. Hence Standard Portland cement, hydrated lime (Calcium Hydroxide) and river sand were used in the mortar.

Table 4 - Average material properties

		0:1:3 mix		1:2:9 mix		
Parameter	**Symbol**	**Strength (MPa)**	**COV (%)**	**Strength (MPa)**	**COV (%)**	**Test method**
Mortar compression	f'_j	0.25 (7)	26	3.2 (5)	33	ASTM C109/C109M-02
Brick compression	f'_b	26.4 (10)	22	26.4 (10)	22	ASTM C67-03a
Masonry compression	f'_m	5.60	-	15.5	-	Almesfer et al. (2014)
Masonry bond	f'_{fb}	0.08	-	0.10	-	
Cohesion	c	0.1	-	0.5	-	
Coefficient of friction	μ	0.65	-	0.65	-	

(#) – number of samples tested

6.4 Test setup

6.4.1 Shake table

The shake table used for testing was relatively simple and cost effective to assemble. Low friction sliders were installed on the underside of the shake table to reduce the friction of the system and to guide the table in a straight line. The harmonic motion of the shake table was controlled by using a flywheel that was attached to the driveshaft of the electric motor, with the flywheel designed such that the table displacement was able to be varied between 35 mm to 80 mm. The shake table was connected to the flywheel with a 20 mm high tensile threaded rod which was also adjustable, to allow the shake table to be centered on the tracks if the table displacement was to be changed.

For all the wall tests, the harmonic motion of the shake table was applied with increasing acceleration every 10 seconds (see **Figure 36** for a typical table input). For each wall test the table acceleration was increased by increasing the speed of the electric motor by 0.5 Hz every 10 seconds, starting from 2.5 Hz. The amplitude of table motion remained constant at 50 mm.

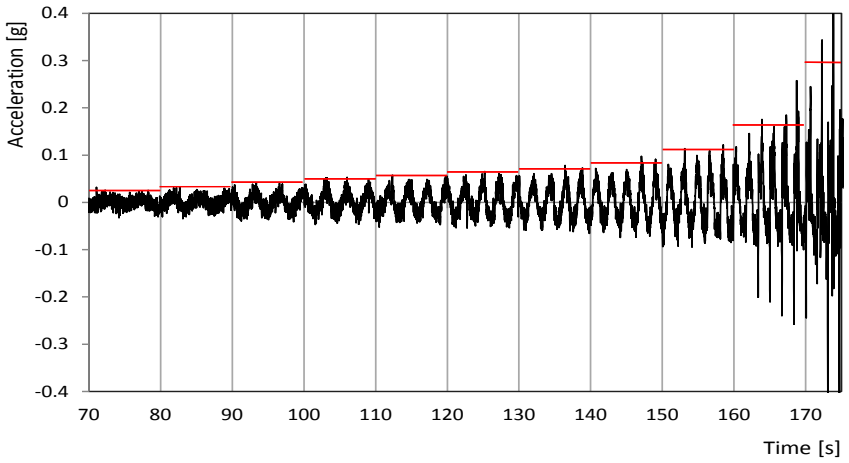

Figure 36 - Typical shake table input used for testing, with solid red lines indicating increasing increments of acceleration

6.4.2 Protection frames & restraints

Two protection frames were designed and built onto the shake table platform, in order to provide wall top restraint and to protect testing instrumentation (see **Figure 37** and **Figure 38**). The design load for the protection frames was based on a conservative estimate of the impact load from the collapsing wall.

(a) Schematic of test setup design

(b) Close up of top part of proposed test setup

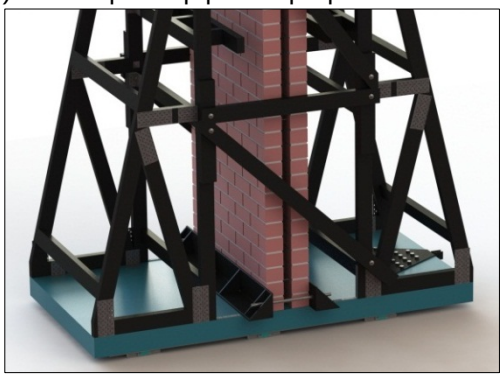

(c) Close up of bottom part of the test setup

Figure 37 - Schematic design of the test setup

(a) Construction of protection frames (b) Assembled protection frames (c) Overall test setup

Figure 38 - Test setup dimensions and construction of protection frames

The protection frames were 300 mm higher than the test wall in order to accommodate the flexible hinge restraint that enabled the top of the wall to freely rotate and uplift after major cracks formed and rocking of the wall was initiated (see **Figure 39**). Two stiff steel angles were used to restrain the wall at the base, and grout was used to fill any gaps between the wall and the angles to ensure that lateral movement of the wall base was not possible (see **Figure 40c**).

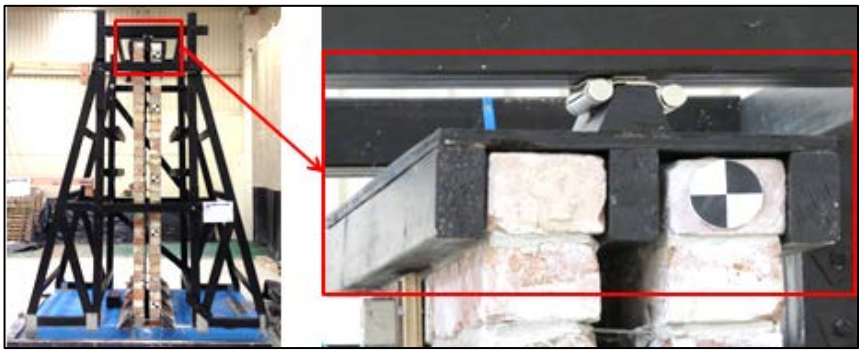

Figure 39 – Close up of typical top wall boundary restraints for walls W1 and W2, showing rotating hinge

The top wall restraint was later adjusted for wall tests W2.2, W3.1, W4.1, and W4.2 using horizontal beams applied to both sides of the wall and in the cavity in order to enable rotations and prevent horizontal translations of the top support (see **Figure 39** and **Figure 40c**). The flexible hinge top restraint was removed after being damaged during test W2.1 and a simplified restraint was adopted for the remaining tests, as shown **Figure 40b**.

(a) Top wall restraint, W1-W2 (b) Top wall restraint, W3-W4 (c) Bottom wall restraint, all

Figure 40 – Typical wall boundary restraints

Wall collapse prevention stoppers were designed and installed onto the protection frames to prevent excessive wall displacements that would have led to complete collapse of the tested wall. Wall collapse was prevented to avoid possible damage of the equipment and instrumentation (see **Figure 41**).

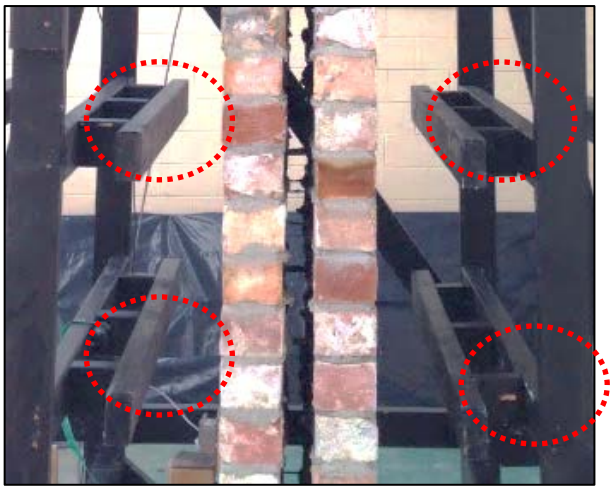

Figure 41 – Wall collapse prevention stoppers (highlighted in red)

6.4.3 Instrumentation

Figure 42 show different types of instruments that were used for the shake table experimental testing. Four accelerometers were installed in specified positions to measure the accelerations of the cavity wall and shake table, and three draw wires were attached to measure the differential displacement of the wall when subjected to horizontal motion. The draw wires were attached to an independent instrumentation frame positioned away from the shaking platform. The instruments were located horizontally at the centre of the test walls and shake table platform, and the vertical positions of the instrumentation relative to the base of the wall are shown in **Table 5**.

(a) Typical accelerometer

(b) Draw wire to measure displacement

Figure 42 – Instrumentation used

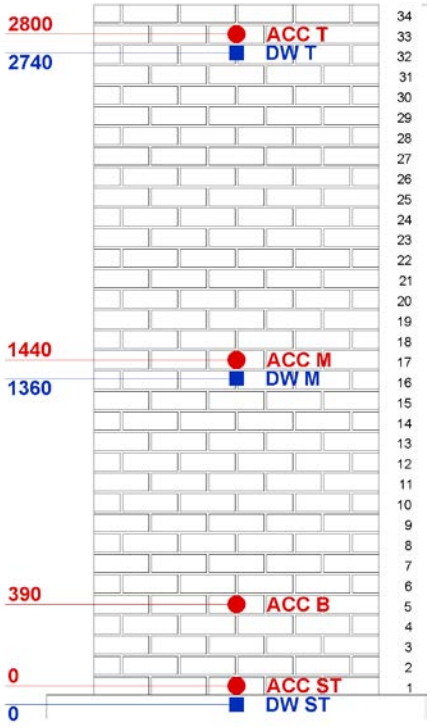

Schematic of instrumentation locations

Table 5 - *Instrument positions (see figure to the left)*

Instrument	***Distance from wall base (mm)***
Top accelerometer (ACC T)	2800
Mid-height accelerometer (ACC M)	1440
Near-table accelerometer (ACC B)	390
Table accelerometer (ACC ST)	0
Top draw wire (DW T)	2740
Mid-height draw wire (DW M)	1360
Table draw wire (DW ST)	0

6.5 Experimental results and discussion

This section presents the results of dynamic shake table testing. General visual observations from wall tests are presented, followed by a detailed analysis and discussion of numerical test data.

A typical displacement history is shown in **Figure 43**. **Figure 44** presents a typical example of relative displacement of the test wall at mid-height where various stages of wall behaviour are indicated and are referred to in the subsequent sections.

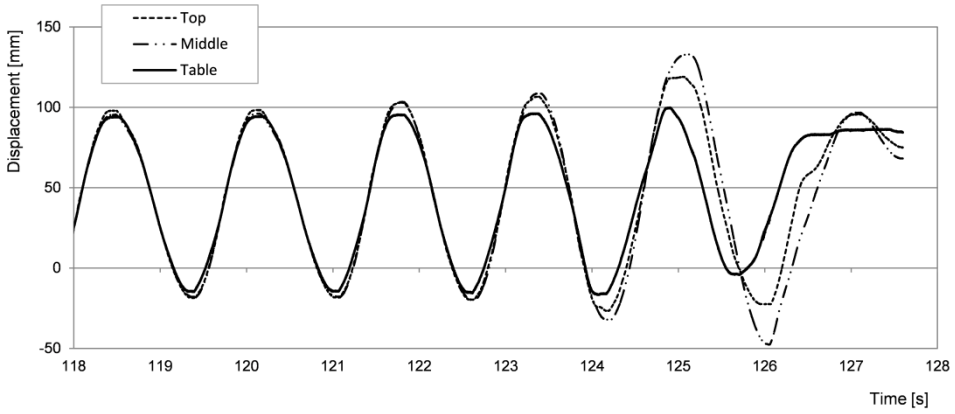

Figure 43 – Representative window of displacement-time history (wall W1.1)

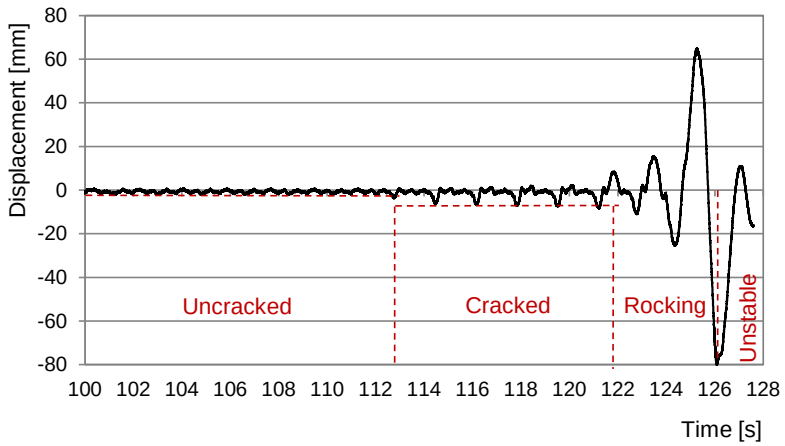

Figure 44 – Typical relative displacement versus time for mid-height of test wall W1.1

6.5.1 Crack patterns

Cracking was mainly concentrated in the top of the walls, involving approximately the top quarter of the wall height. The following figures show screenshots of failure propagation and the associated crack-pattern for each tested wall. For all test walls, cracks and failure areas marked in red were detected during the initial test, while cracks marked in black and areas marked grey were observed following the subsequent test (except for wall W3, where only one test was conducted).

Differential movement of the two wall layers was observed in as-built wall W1. At the failure state it was observed that the width of the cavity between the two wall layers was significantly reduced, indicating the low compressive strength of the original cavity ties, see **Figure 45b,c**. In addition, the relative displacement capacity of wall W1 was limited due to weak mortar strength and major cracks fully opened following a few cycles of stable rocking during the W1.1 test (see **Figure 45a**). Following the second test (W1.2), no additional cracks were observed but collapse at the top of the one of the masonry layers occurred (see **Figure 45**).

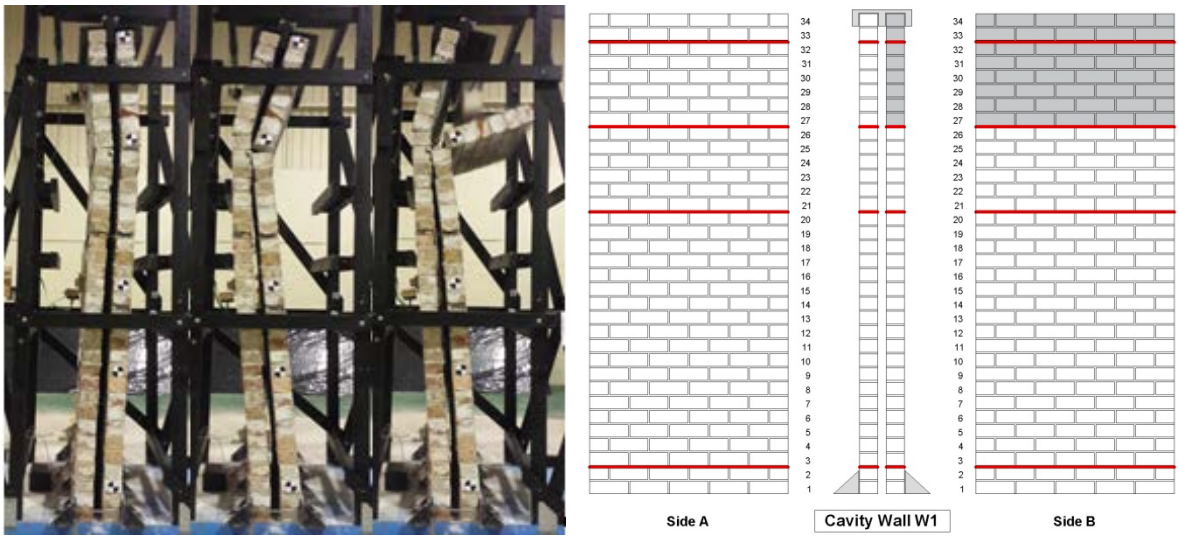

(a) (b) (c) (d)

Figure 45 - Wall W1 screenshots showing failure progression and crack-pattern survey

During the process of installing mechanical screw ties as a retrofit for wall W2, two screw ties were accidentally omitted in course 4 (compare **Figure 35a** and **Figure 46d**) and this had an influence on the failure mode. The retrofitted wall W2 failed in a similar manner as the as-built W1 wall, but the mid-section acted compositely as a rigid body. During test W2.1 two masonry courses at the top collapsed and the top restraint was modified (see **Figure 40b** and **Table 3**). A crack appeared between courses #8 and #9, corresponding to the location of the lowest row of retrofit screw ties that were applied. Due to the absence of ties in the top three masonry courses, the width of the cavity between the two wall layers was significantly reduced at the top of the wall (see **Figure 46a,b** also refer to red section in **Figure 46d**). Wall W2 became unstable during test W2.2 as the displacement capacity of the bottom section of the wall was exceeded, leading to a 'soft storey' type of collapse as shown in **Figure 46c**.

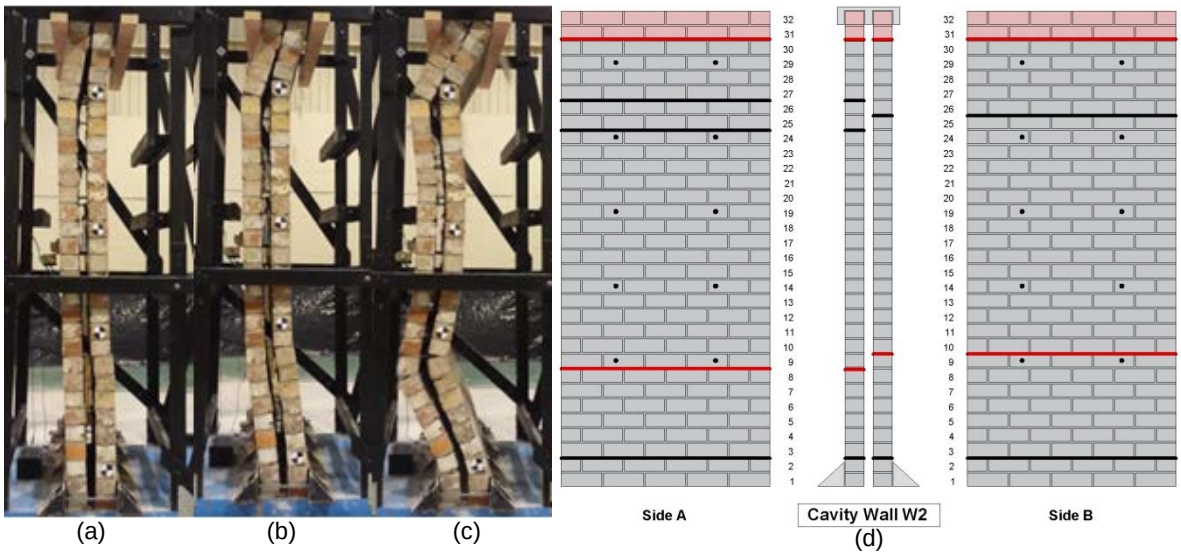

(a) (b) (c) (d)

Figure 46 - Wall W2 screenshots showing failure progression and crack-pattern survey

During the W3.1 test the wall responded as a rigid body (see **Figure 47**). Due to increasing bending and shear from uplift and rotation in conjunction with rocking of the wall, the top section of wall W3 failed because the mortar strength was exceeded. On one side the collapse involved the masonry above the highest row of ties while on the opposite side the failure included two rows of ties (compare Side A and Side B in **Figure 47d**).

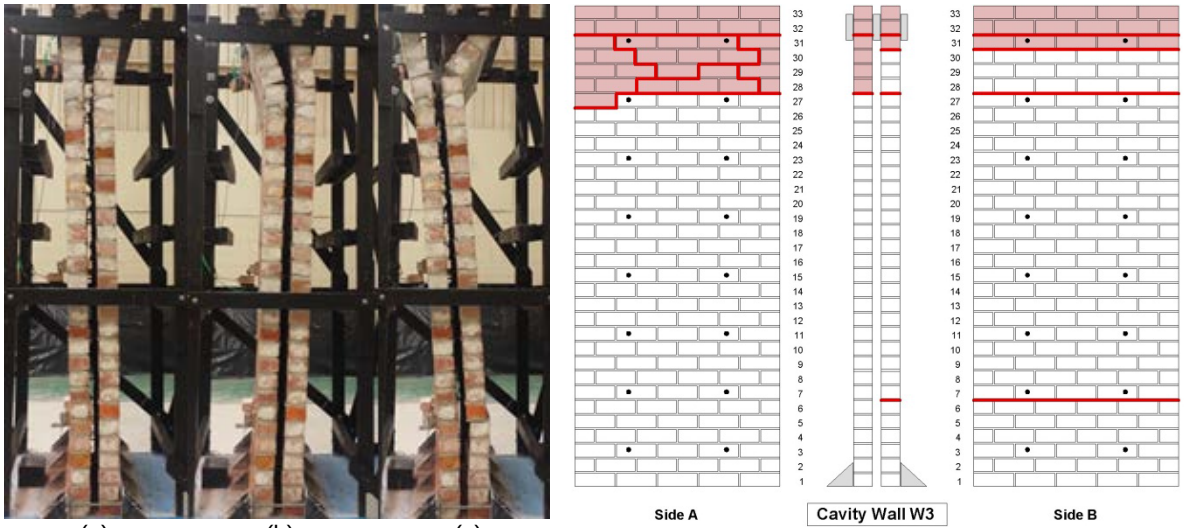

(a) (b) (c) (d)

Figure 47 - Wall W3 screenshots showing failure progression and crack-pattern survey

Wall W4 was initially tested as-built (test W4.1) and developed only one crack at the top of the wall, through both wall layers (**Figure 48a)**. The second test (test W4.2) was carried out following the application of Type 2 ties (see **Figure 33d**) that allowed solid wall type behaviour between wall layers, as shown **Figure 48b,c**. The failure of the retrofitted wall W4.2 occurred at the 25th and 23rd courses while the as-built test crack location occurred at the 30th and 28th courses. Also, an additional crack near the bottom restraint (3rd course) appeared at high levels of table acceleration.

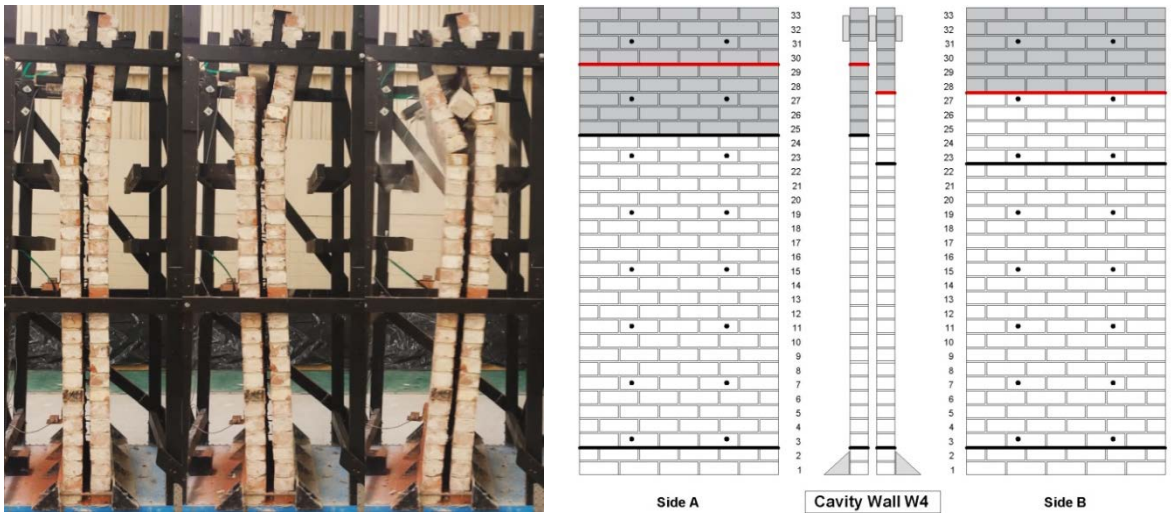

(a) (b) (c) (d)

Figure 48 - Wall W4 screenshots (W4.2) showing failure progression and crack-pattern survey

6.5.2 Wall response

A summary of experimental results is shown below in terms of Peak Ground Acceleration (PGA) and horizontal relative displacement of the test walls. **Figure 49** shows the PGA achieved by each wall at two different stages of wall behaviour, where the hatch pattern fill (W1.1 and W4.1) indicates the as-built walls. PGA achieved for initial cracking is shown as hatched in light grey and PGA corresponding to the initiation of rocking is shown as hatched in dark grey for each wall tested. Significant improvements in PGA were also registered for the retrofitted walls W2.1 and W3.1, with an increase in PGA of 40-50%. Wall W2.1 experienced a lower PGA at the initial wall cracking stage in comparison to wall W1.1 and W3.1, as shown **Figure 49**. This lower PGA was mainly attributed to the premature cracking of W2.1 that occurred at the top support, as indicated by the red hatched area in **Figure 46d**.

W4.1 was constructed using stronger mortar that resulted in the wall reaching a 30% higher PGA (0.59g) than was achieved for wall W1.1 (0.45g). The peak capacity of the cavity walls increased when retrofit screw ties were installed (W2.1, W3.1, and W4.2), with the magnitude of increase being inversely related to the tie spacing (W3.1 and W4.2). Walls with weak mortar (see section 6.1) and Ø12 steel screw ties achieved PGA values of 0.58g for W2.1 and 0.71g for W3.1, with an increment of approximately 30% and 60% above the capacity of as-built wall W1.1. Wall W4 was constructed with stronger mortar (see section 6.1) and Ø8 screws ties (Type 2) and reached a PGA of 1.00g, being 70% higher than the capacity of the as-built wall W4.1.

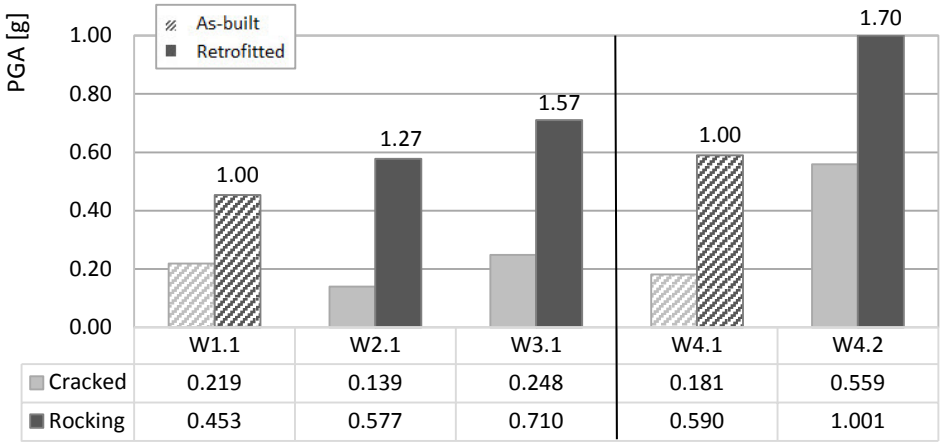

	W1.1	W2.1	W3.1	W4.1	W4.2
Cracked	0.219	0.139	0.248	0.181	0.559
Rocking	0.453	0.577	0.710	0.590	1.001

Figure 49 - PGA achieved for initial cracking (hatched in light grey) and initiation of rocking (hatched in dark grey) for each wall tested (values at the top of each column indicate ratio of improvement relative to appropriate as-built test)

An in-depth analysis enabled the amplification of the peak acceleration vs wall height and the lateral displacement vs wall height to be identified, with the acceleration values normalized with respect to the table PGA in order to simplify the comparison between the walls. As a first step, these analyses were carried out at three stages of the test corresponding to the three main conditions of the test wall: (1) uncracked, (2) cracked, and (3) rocking, see **Figure 50**. In **Figure 50a** it is shown that the acceleration profile was relatively constant in the uncracked condition, and

that as cracking occurred the acceleration profile becomes more triangular with the maximum acceleration developing at the wall mid-height, see **Figure 50c**. Following the initiation of rocking, the mid-height acceleration significantly decreased, resulting in smaller acceleration than that of the table, see **Figure 50e**. The window of displacement-time and acceleration-time history for each analysed stage of wall behaviour is also presented in **Figure 50b-d-f** for each respective stage of wall behaviour.

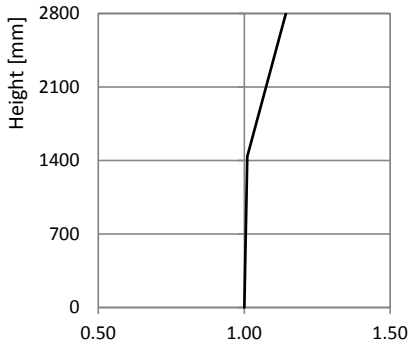

(a) Uncracked behaviour

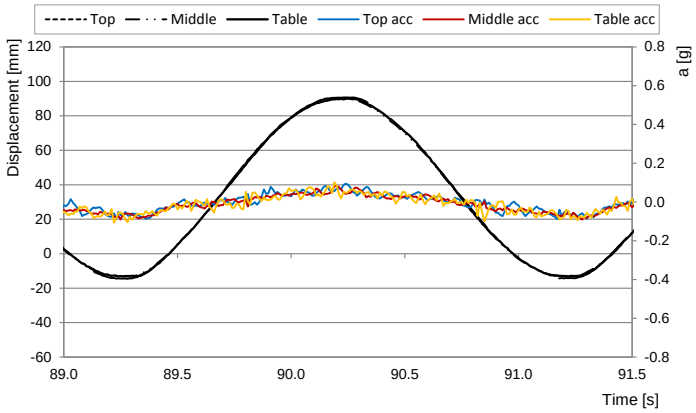

(b) Representative window of displacement-time and acceleration-time history for uncracked behaviour

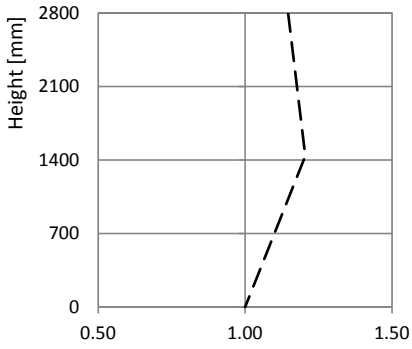

(c) Cracked behaviour

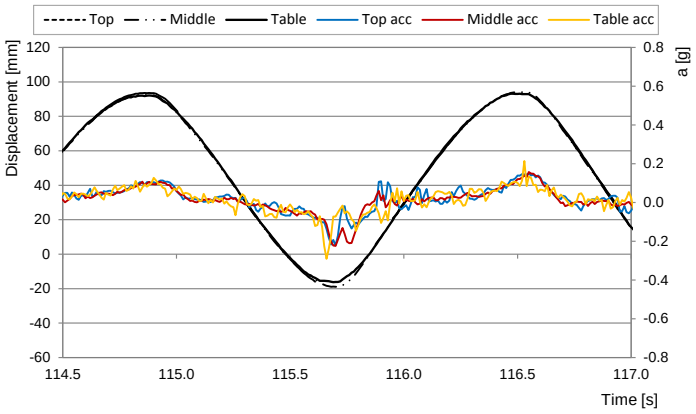

(d) Representative window of displacement-time and acceleration-time history for cracked behaviour

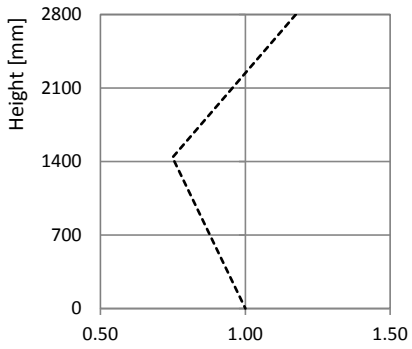

(e) Rocking behaviour

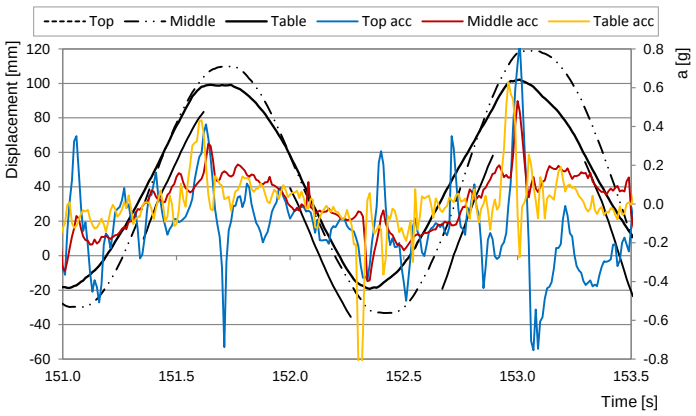

(f) Representative window of displacement-time and acceleration-time history for rocking behaviour

Figure 50 – Typical acceleration amplification vs wall height at different stages for wall W3.1

A comparison between all the test walls considering only the acceleration profile at the final stage of the test (such as immediately prior to collapse) is shown in **Figure 51**. All walls exhibited an acceleration decrease at the middle of the panel that ranged between 25% of the PGA for W4.1, 50% for W1.1 and W1.2, and 70% for W3.1 and W4.1.

At the top of the walls with weak mortar (W1.1 and W3.1) the recorded acceleration was 120% of the table PGA (**Figure 51a**), and for walls with stronger mortar (W4.1 and W4.2) the recorded acceleration was 85% of the table PGA (**Figure 51b**). The data recorded at the top of W2.1 was affected due to the damage pattern that resulted in cantilever type behaviour. This cantilever wall behaviour is clearly shown in the displacement graph in **Figure 52a**.

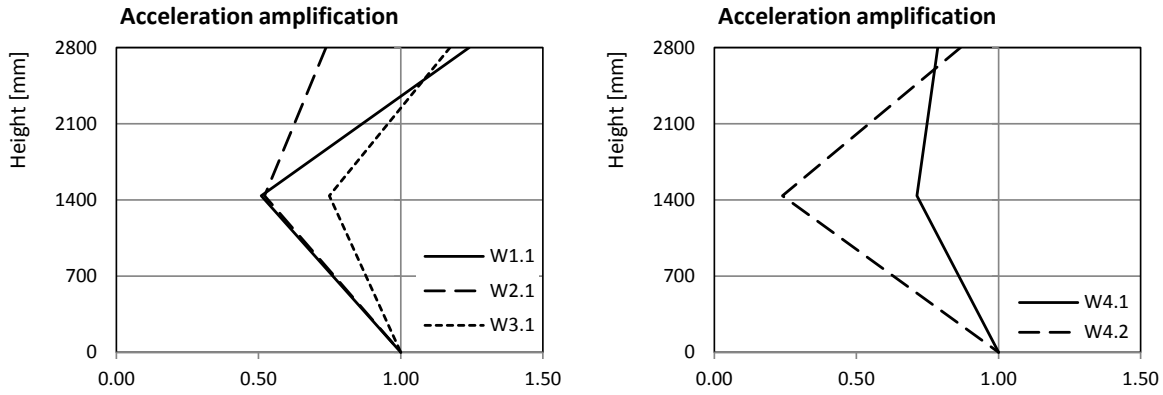

(a) Mortar 1:3 and Ø12 steel (Type 1) screws (b) Mortar 1:3:9 and Ø8 (Type 2) screws

Figure 51 – Peak acceleration vs wall height normalized with respect to the table acceleration (data from W1.2 and W2.2 is not presented due to the malfunction of top accelerometer)

Table 6 summarises the peak acceleration values in g recorded respectively at bottom, middle and top of each test wall.

Table 6 – Peak acceleration vs wall height

ID	Height (mm)	W1.1 (g)	W1.2 (g)	W2.1 (g)	W2.2 (g)	W3.1 (g)	W4.1 (g)	W4.2 (g)
Top	2800	0.562	n/a	0.426	n/a	0.833	0.464	0.867
Middle	1440	0.230	0.186	0.301	0.377	0.532	0.420	0.239
Bottom	390	0.453	0.238	0.577	0.953	0.710	0.590	1.001

Figure 52 presents the relative lateral displacement of the wall vs height, indicating that the walls behaved as vertically oriented 'simply supported beams'. The maximum mid-height displacement that occurred in the walls with weak mortar (W1.1 and W3.1, **Figure 52a**) was approximately 26-27 mm and the top displacement of W3.1 was approximately double that for W1.1 at 30 mm.

During the second test, as-built W1.2 developed the same displacements as that recorded in W3.1 at the first test, with a registered acceleration at the middle and top that was 80% of the table PGA. Considering the test walls with stronger mortar (W4.1 and W4.2, **Figure 52b**), rigid body behaviour was observed with the maximum displacement being similar at mid-height and top of the as-built wall, being 18 mm and 16 mm respectively. The addition of Type 2 screws ties resulted in accelerations that were higher than those developed by the as-built wall, with a maximum mid-height displacement of 65 mm and a 23 mm displacement at the top of the wall.

Table 7 summarises the maximum displacement values in mm recorded respectively at the bottom, mid-height and top of each tested wall.

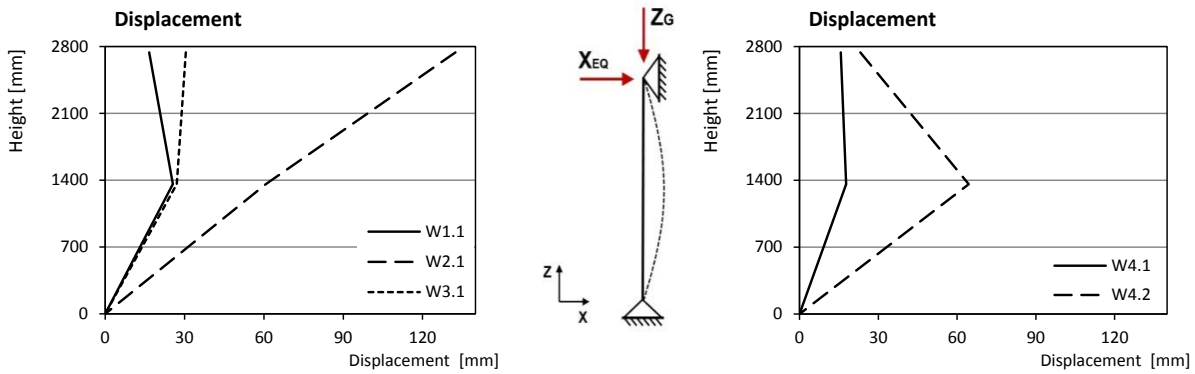

(a) Mortar 1:3 and Ø12 steel screws (Type 1)

(b) Mortar 1:3:9 and Ø8 screws (Type 2)

Figure 52 – Displacement vs wall height and design static scheme

Table 7 – Displacement vs wall height

Wall ID	Height (mm)	W1.1 (mm)	W1.2 (mm)	W2.1 (mm)	W2.2 (mm)	W3.1 (mm)	W4.1 (mm)	W4.2 (mm)
Top	2740	16.61	29.37	132.42	n/a	30.46	15.68	23.20
Middle	1360	25.55	22.73	60.75	105.52	27.07	17.76	64.48

As a final analysis, the trend of displacement versus the increase of PGA was evaluated both at mid-height and at top of the test walls. **Figure 53** and **Figure 54** represent respectively the data collected in the walls with weak mortar (W1.1, W2.1, and W3.1) and in the walls with stronger mortar (W4.1 and W4.2). The PGA and displacement registered at initial cracking are indicated with blue marks, while the rocking and consequent collapse at the maximum PGA is indicated by red marks. Large displacements were achieved at relatively small PGA in all the as-built walls. Both in W1.1 and W4.1 the initial cracking was observed at approximately 0.20g, corresponding to approximately 3 mm of displacement at the mid-height and 5 mm of displacement at the top of the walls. For retrofitted walls W2.1, W3.1 and W4.2, cracking initiated at 0.14g, 0.25g, and 0.56g respectively, with displacement at the mid-height ranging between 0.05 to 1.84 mm and between 0.4 to 3.5 mm of displacement at the top of the walls. Based on the displacement at failure, the

wall mid-height displacement were similar to W1.1, W1.2 and W4.2, with a value of approximately 26 mm. Wall W4.1 exhibited a mid-height displacement of 10 mm due to the higher mortar strength when compared to walls W1-W3 and at the top of the wall, displacement and PGA values were significantly different due to the increase of the motion with increasing height of the wall.

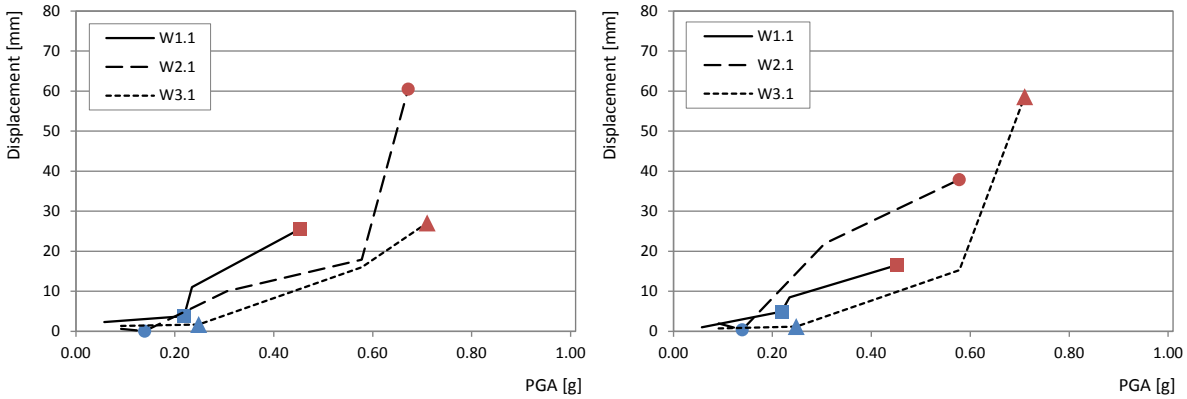

(a) Middle (b) Top

Figure 53 – PGA vs maximum displacement recorded in the walls with mortar 1:3 and Ø12 steel screws (Type 1), W1.1, W2.1 and W3.1

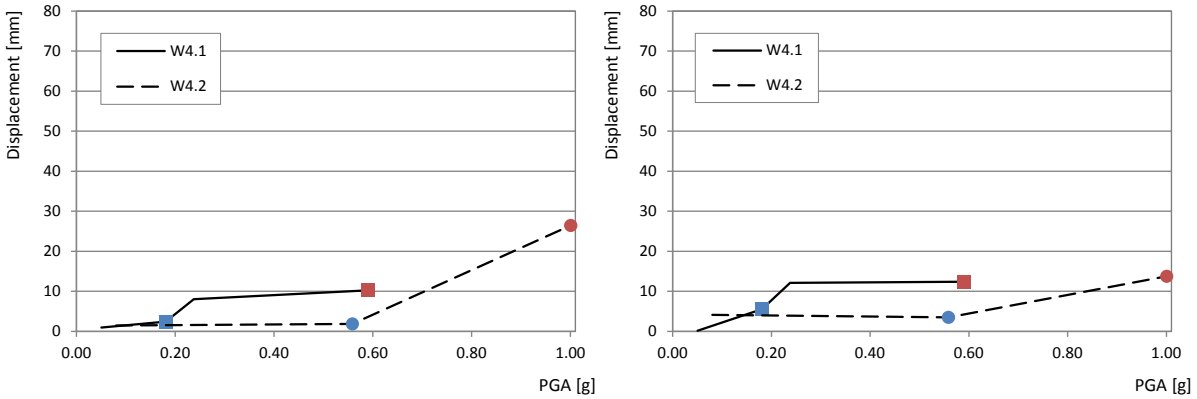

(a) Middle (b) Top

Figure 54 – PGA vs maximum displacement recorded in the wall with mortar 1:3:9 and Ø8 screws (Type 2), W4.1 and W4.2

The average wall period was calculated for each test wall, with the results presented in **Table 8**. The period of the test walls was calculated based on the average of at least three stable cycles of wall rocking using the mid-height relative displacement.

The average period of Wall W1 increased from 1.66 sec to 2.14 sec with increasing mid-height displacement. This increased wall period was attributed to greater observed damage, differential movement between the wall layers, and deterioration of the mortar joints at the rocking plane. Wall periods decreased with increasing level of retrofit. For W2 (retrofitted using Type 1 screw ties at 600 x 600 mm spacing) the wall period was 1.56 sec and for W3 (retrofitted using Type 1 screw ties at 600 x 300 mm spacing) the wall period was 1.37 sec . This reduced period with comparison

to the as-built wall W1 was attributed to the ability of the retrofitted wall layers to act as interconnected elements that resulted in increased rocking wall thickness. As-built wall W4 with higher mortar compressive strength compared to W1-W3 had an average rocking period of 1.30 sec. The higher rocking period was attributed to relatively high mortar compressive strength and the ability of the wall to rock without severe deterioration of the mortar joints at the rocking plane, as was observed for wall W1. The average rocking period of wall W4 decreased to 1.10 sec following installation of Type 2 screw ties at 600 x 300 mm spacing.

Table 8 - Average rocking period of walls

Test ID	Average period (sec)	Retrofit type	Mortar type
W1.1	1.66	Original	0:1:3
W1.2	2.14		
W2.1	n/a	Type 1	
W2.2	1.56		
W3.1	1.37		
W4.1	1.30	Original	1:2:9
W4.2	1.10	Type 2	

Mortar type - cement : lime : sand

7. Future research opportunities

The shake table testing reported here used a simplified experimental set-up to apply harmonic motion. This testing should be extended using a more sophisticated experimental set-up and scaled records of actual earthquake ground motions. Further work is also required to quantify the extent of improvement when using mechanical screws as a seismic retrofit solution for URM cavity wall construction, so that an engineering calculation procedure can be developed to enable detailed seismic assessment to be undertaken, ultimately leading to the establishment of a %NBS score.

8. Conclusions

Because the original design of URM cavity wall type construction did not account for earthquake induced loading, cavity walls have limited seismic capacity as has been repeatedly illustrated in past earthquakes. It was found that cavity walls in their original state make up approximately 40% of New Zealand URM buildings, with the remainder having solid interconnected multi-leaf walls. Based on a detailed review of 125 documented URM cavity wall buildings that were damaged during the 2010/2011 Canterbury earthquakes it was concluded that unretrofitted URM cavity walls generally suffered irreparable damage due to weak mortar strength and lack of effective wall restraints. The majority (approximately ¾) of the observed damage was a result of out-of-plane type wall failures. Three types of out-of-plane wall failures that were commonly observed in cavity walls are:

- Cantilever type failure with the entire top section of a wall or building façade collapsing (36%)
- One-way bending type failure, which tended to occur in long spanning walls and/or walls without side support (7%)
- Two-way bending type failure, which tended to occur in walls restrained at all boundaries (57%)

In-plane damage of URM cavity walls was less widely observed (approximately ¼) than out-of-plane damage and commonly included:

- Diagonal shear cracking in piers, spandrels and walls
- Shear sliding on mortar bed joints or between building storeys.

Based on detailed investigation of earthquake damaged buildings in Christchurch, it was concluded that original cavity wall ties were typically corroded due to moisture ingress. The badly corroded wall ties further deteriorated the lateral loadbearing capacity of cavity walls and their resistance to shear and flexural actions. It was revealed that the most commonly encountered ties were horse-toe steel wire ties, having a cross-section that was typically found to be significantly reduced due to corrosion at the mortar bed joints. Pull-out of the original ties from the mortar joints was also observed. The spacing arrangement of the cavity ties was observed to be three bricks horizontally and six bricks vertically in most cases. Further field investigations also confirmed the rusted condition of wall ties in URM cavity wall buildings located in the Auckland area.

Shake table testing was undertaken on four full scale URM cavity walls. As-built wall W1 achieved a PGA of 0.45g, while retrofitted walls W2 and W3 reached a PGA of 0.58g and 0.71g respectively, resulting in 30% and 57% improvement respectively. Wall W4 was constructed using stronger mortar that led to the wall reaching a 30% higher PGA (0.59g) than W1, in the as-built

condition. The PGA achieved in retrofitted wall W4.2 was 1.00g, being 70% higher than the as-built test W4.1.

For all walls, the crack-pattern was mainly concentrated in the top quarter of the wall height. The as-built walls clearly showed the low strength of original ties and their ability to provide composite action between the wall layers. Retrofitted walls mainly resulted in composite behaviour of the two wall layers, leading to rigid body behaviour. This rigid body behaviour was confirmed based on analysing the horizontal displacement data. Highest displacements occurred in the test walls with weak mortar.

In all as-built walls (W1.1 and W4.1), high displacements were reached at relatively small PGA values. The initial cracking was observed at approximately 0.20g, corresponding to a 3 mm mid-height displacement and a 5 mm displacement at the top of the walls. The retrofitted walls W2.1, W3.1 and W4.2 initiated cracking at 0.14g, 0.25g, and 0.56g respectively, with mid-height displacements of less than 2 mm.

9. Acknowledgments

The authors wish to thank the numerous professional structural engineers and building owners who have provided valuable data and shared their opinions, expertise and experiences related to this study. The authors also thank and recognise the efforts by Marta Giaretton, Chengliang Qian and Kevin Jiang during this project. The authors acknowledge financial support from BRANZ and the New Zealand Natural Hazards Research Platform.

10. References

Adams, H., 1846-1935. (1908). "Building Construction: Comprising Notes on Materials, Processes, Principles, and Practice", Cassell and Co. London.

Almesfer, N., Dizhur, D., Lumantarna, R., and Ingham, J. (2014) 'Material Properties of Existing Unreinforced Clay Brick Masonry Buildings in New Zealand'. Bulletin of the New Zealand Society for Earthquake Engineering, 47(2)

ASTM (2003). "Standard Test Method for Compressive Strength of Masonry Prisms." C 1314-03b, ASTM International, Pennsylvania, United States.

ASTM (2003b). "Standard Test Methods for Sampling and Testing Brick and Structural Clay Tile." C 67 - 03a, ASTM International, Pennsylvania, United States.

ASTM (2008a). "Standard Specification for Mortar for Unit Masonry." C 270 - 08a, ASTM International, Pennsylvania, United States.

ASTM (2000). "Standard Test Method for Measurement of Masonry Flexural Bond Strength." C 1072 -00a, ASTM International, Pennsylvania, United States.

Dearn, T. (1821). "Hints on an Improved Method of Building". England.

Dickey, J. M. (1974). "Introduction to Early American Masonry, Stone, Brick, Mortar and Plaster (book review)" DOI: 10.2307/1493406.

Dizhur, D., Ismail, N., Knox, C., Lumantarna, R., J. M. Ingham, et al. (2010). "Performance of unreinforced and retrofitted masonry buildings during the 2010 Darfield earthquake." Bulletin of the New Zealand Society for Earthquake Engineering 43(4): 321-339.

Dizhur, D., Ingham, J. M., Moon, L., Griffith, M. C., Schultz, A., Senaldi, I., Lourenco, P. (2011). "Performance of Masonry Buildings and Churches in the 22 February 2011 Christchurch Earthquake". Bulletin of the New Zealand Society for Earthquake Engineering, Vol 44, No. 4, pp. 279-296.

Downing, A. J. (1850). "Architecture of Country Houses". University of Virginia Library. New York. DOI:NA7561 D75 1850

Dowrick, D. J. (1996). "The Modified Mercalli Earthquake Intensity Scale - Revisions Arising from Recent Studies of New Zealand Earthquakes". Bulletin of the New Zealand Society for Earthquake Engineering. Vol 29, No. 2, pp.92-106.

Eveleigh, D. (2009). "Evolution of Building Elements". University of the West of England, Bristol, England. Retrieved on 10th June 2014 Available from: http://fet.uwe.ac.uk/conweb/house_ages/elements/print.htm

Griffith, M. C. (1991). "Performance of Unreinforced Masonry Buildings during the Newcastle Earthquake, Australia". University of Adelaide, Australia. No. R86.

Gwilt, J. (1888). "An Encyclopaedia of Architecture, Historical, Theoretical and Practical". Longmans, London. DOI:AEQ-1401.

Hamilton, S. B. (1958). "The History of Hollow Bricks". Transactions, British Ceramic Society, Vol 58, No. 2.

Ingham, M. J., Walsh, K., Dizhur, D., & Shafaei, J. (2014). "Out-of-plane Testing of Unreinforced Brick Infill Walls within Structural Frames". The University of Auckland, New Zealand. No. LR0441.

Ingham, J. M., & Griffith, M. C. (2011). "The Performance of Unreinforced Masonry Buildings in the 2010/2011 Canterbury Earthquake Swarm". Addendum Report to the Royal Commission of Inquiry. No. ENG.ACA.0001F.

Klingner, R. E., Masonry Society (U.S.) Investigating Disasters Reconnaisance Team. (1994). "Performance of Masonry Structures in the Northridge, California Earthquake of January 17, 1994". [Boulder, Colo.], Masonry Society.

Lewis, M. (1998). "Australian Building: A Cultural Investigation", Bricks and tiles.

McKenzie, W. (2001). "Wall ties". Design of Structural Masonry, Palgrave Macmillan, UK. pp. 15-16.

Monk, C. B. (1960). "Insulated Masonry Cavity Walls". Retrieved on 15th June 2014 Available from: http://books.google.co.nz/books

Nicholson, P. (1852). "Architectural Dictionary". [Lomax, Gunyon.], England.

Nasseri A. (2012). AIR Worldwide. "Assessing the Seismic Vulnerability of Australia's Building Stock". Retrieved from http://www.air-worldwide.com/Publications/AIR-Currents/2012/Assessing-the-Seismic-Vulnerability-of-Australia%E2%80%99s-Building-Stock/

Newcastle Cultural Collections (2005) Earthquake Database. Retrieved from http://collections.ncc.nsw.gov.au/keemu/pages/nrm/index.htm

NZSS No. 95:1935, Model Building By-law, New Zealand Standards Institute, Wellington, New Zealand, Standard U.S.C. (1935).

Page, A. W. (1996). "Unreinforced Masonry Structures - an Australian Overview". Bulletin of the New Zealand Society for Earthquake Engineering, Vol. 29, No. 4. pp.242-255.

Patel, J. K. (2013). "Securing of Unreinforced Masonry Parapets, Part B: Retrofit Testing". Available from: Department of Civil and Environmental Engineering, University of Auckland, New Zealand.

Pickles, D., Brocklebank, I., & Wood, C. (Eds.). (2010). "Energy Efficiency and Historic Buildings". English Heritage, England.

Qian, C. (2014). "Experimental Testing of Unreinforced Masonry Cavity Walls". Available from: Department of Civil and Environmental Engineering, University of Auckland, New Zealand.

Russell, A. P. (2010). "Characterisation and seismic performance of unreinforced masonry buildings". PhD Thesis, Available from: Department of Civil and Environmental Engineering, University of Auckland, New Zealand.

Ritchie, T. (1961). "Cavity Walls". Retrieved on 20th June 2014, Available from: http://web.mit.edu/parmstr/Public/NRCan/CanBldgDigests/cbd021_e.html

Russell, A. P. and J. M. Ingham (2010). "Prevalence of New Zealand's unreinforced masonry buildings." *Bulletin of the New Zealand Society for Earthquake Engineering* **43**(3): 182-201.

Standards Australia (2001). "Appendix D: Method of Test for Flexural Strength." AS 3700 - 2001, Standards Australia, Homebush, New South Wales, Australia.

Walsh, K. Q., Dizhur, D. Y., Almesfer, N., Cummuskey, P. A., Cousins, J., Derakhshan, H., Griffith, M. C., Ingham, J. M. (2014) 'Geometric characterisation and out-of-plane seismic stability of low-rise unreinforced brick masonry buildings in Auckland, New Zealand', Bulletin of the New Zealand Society for Earthquake Engineering, 47, 2, June, 139-156.

University of the West England (2013). Cavity Wall Insulation. Retrieved December 2014, from http://www.uwe.port.ac.uk/hi4web/cavity%20walls/index.htm